JACS
JOURNAL OF THE AMERICAN CHEMICAL SOCIETY

ARTICLE

pubs.acs.org/JACS

Convergent Synthesis of Homogeneous $Glc_1Man_9GlcNAc_2$-Protein and Derivatives as Ligands of Molecular Chaperones in Protein Quality Control

Mohammed N. Amin, Wei Huang, Rahman M. Mizanur, and Lai-Xi Wang*

Institute of Human Virology, Department of Biochemistry & Molecular Biology, University of Maryland School of Medicine, Baltimore, Maryland 21201, United States

Supporting Information

ABSTRACT: A detailed understanding of the molecular mechanism of chaperone-assisted protein quality control is often hampered by the lack of well-defined homogeneous glycoprotein probes. We describe here a highly convergent chemoenzymatic synthesis of the monoglucosylated glycoforms of bovine ribonuclease (RNase) as specific ligands of lectin-like chaperones calnexin (CNX) and calreticulin (CRT) that are known to recognize the monoglucosylated high-mannose oligosaccharide component of glycoproteins in protein folding. The synthesis of a selectively modified glycoform $Gal_1Glc_1Man_9GlcNAc_2$-RNase was accomplished by chemical synthesis of a large N-glycan oxazoline and its subsequent enzymatic ligation to GlcNAc-RNase under the catalysis of a glycosynthase. Selective removal of the terminal galactose by a β-galactosidase gave the $Glc_1Man_9GlcNAc_2$-RNase glycoform in excellent yield. CD spectroscopic analysis and RNA-hydrolyzing assay indicated that the synthetic RNase glycoforms maintained essentially the same global conformations and were fully active as the natural bovine ribonuclease B. SPR binding studies revealed that the $Glc_1Man_9GlcNAc_2$-RNase had high affinity to lectin CRT, while the synthetic $Man_9GlcNAc_2$-RNase glycoform and natural RNase B did not show CRT-binding activity. These results confirmed the essential role of the glucose moiety in the chaperone molecular recognition. Interestingly, the galactose-masked glycoform $Gal_1Glc_1Man_9GlcNAc_2$-RNase also showed significant affinity to lectin CRT, suggesting that a galactose β-1,4-linked to the key glucose moiety does not significantly block the lectin binding. These synthetic homogeneous glycoprotein probes should be valuable for a detailed mechanistic study on how molecular chaperones work in concert to distinguish between misfolded and folded glycoproteins in the protein quality control cycle.

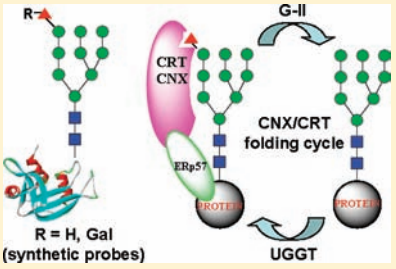

INTRODUCTION

Asparagine (N)-linked glycosylation is an important co- and post-translational modification of proteins in eukaryotic cells. Recent studies have suggested that the attached high-mannose type N-glycans with subtle structural difference play a pivotal role in various steps of the protein quality control process, including the calnexin (CNX)/calreticulin (CRT)-mediated protein folding and the endoplasmic reticulum (ER)-associated protein degradation pathways.[1] N-Glycosylation occurs when a tetradecasaccharide precursor, $Glc_3Man_9GlcNAc_2$, is transferred by an oligosaccharyltransferase (OST) from a sugar-lipid precursor to an asparagine side chain in the consensus Asn-X-Ser/Thr sequon of a nascent polypeptide (where X can be any amino acid except proline). The precursor is then processed by ER α-glucosidases I and II (G-I and G-II) to di- and monoglucosylated glycoforms, respectively. The monoglucosylated form, $Glc_1Man_9GlcNAc_2$ (Glc, glucose; Man, mannose; GlcNAc, *N*-acetylglucosamine), is an essential ligand recognized by molecular chaperones calnexin (CNX) and calreticulin (CRT). Upon binding to the monoglucosylated glycoform, CNX and CRT recruit other molecular chaperones such as protein disulfide isomerase-like protein ERp57 to form a complex for appropriate folding. Once the last Glc residue is removed by α-glucosidase II (G-II), the resulting $Man_9GlcNAc_2$-protein will be released from the CNX/CRT folding cycle. At this point, an ER-residing UDP-glucose:glycoprotein glucosyltransferase (UGGT) serves as a "folding sensor" to detect and reglucosylate the misfolded or partially folded protein to generate the monoglucosylated glycoform, which enters into the CNX/CRT cycle again for refolding (Figure 1).[1,2] Despite tremendous efforts in this field, the molecular mechanism of the protein quality control process that involves a number of specific protein−carbohydrate interactions is still not fully understood. A major obstacle is the difficulty to obtain homogeneous, structurally well-defined glucosylated N-glycoproteins for detailed mechanistic and functional studies.[3−5] As an elegant chemical approach, Ito and co-workers have synthesized an array of monoglucosylated high-mannose type N-glycans and derivatives, and used them as probes to study their interactions with lectin-like chaperones.[6,7] Nevertheless, preparation of related homogeneous natural glycoproteins, which are highly desirable as probes for understanding how a

Received: May 26, 2011
Published: August 06, 2011

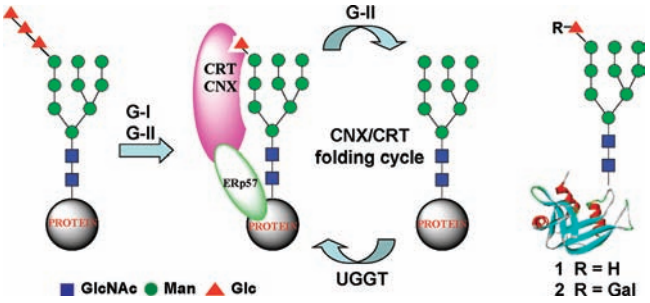

Figure 1. The clnexin/calreticulin-assisted folding cycle and the structures of synthetic glycoprotein probes (**1**) and (**2**).

specific oligosaccharide and the misfolded protein domain act in concert to provide the right signal for folding, is much more challenging. Some of the glycoforms may be only transiently present in the quality control process and are extremely difficult to isolate from natural source. For example, in a classic study on calnexin-mediated protein folding using bovine ribonuclease B (RNase B) as the model glycoprotein, the monoglucosylated RNase B was prepared through in vitro glucosylation of a mixture of denatured RNase B glycoforms (ranging from $Man_5GlcNAc_2$-RNase to $Man_9GlcNAc_2$-RNase) using radiolabeled UDP-glucose and enzyme UGGT, which gave only about 2% monoglucosylated RNase B with uncharacterized ratio of the glycoforms.[3] The use of undefined glycoform mixtures as probes complicated the interpretation of the experimental results.

We report here a convergent chemoenzymatic synthesis of homogeneous glycoforms of bovine ribonuclease (RNase), including the monoglucosylated glycoform $Glc_1Man_9GlcNAc_2$-RNase (**1**) and a selectively modified derivative Gal_1Glc_1-$Man_9GlcNAc_2$-RNase (**2**) (Gal represents a galactose moiety). Glycoprotein (**2**), in which the terminal Glc residue is selectively masked by a β-1,4-linked Gal residue, is an unnatural glycoform designed for probing how site-specific modification on the Glc moiety perturbs its recognition by lectin-like molecular chaperones. We also report here the binding of the synthetic glycoforms with molecular chaperone CRT. Our experimental data showed that while nonglucosylated glycoforms, including the natural bovine RNase B ($Man_{5-9}GlcNAc_2$-RNase) and a synthetic high-mannose glycoform $Man_9GlcNAc_2$-RNase, either in the folded or denatured forms, were not recognized by CRT, the synthetic monoglucosylated glycoform (**1**) could bind to CRT with high affinity. Interestingly, the modified monoglucosylated glycoform (**2**) also demonstrated significant binding to lectin CRT.

RESULTS AND DISCUSSION

Retrosynthetic Design of Glycoproteins 1 and 2. Our synthesis was based on a chemoenzymatic approach that was developed by us and others, which employs endoglycosidase-catalyzed transglycosylation for regio- and stereoselective ligation of a synthetic N-glycan (in the form of the activated sugar oxazoline) to a GlcNAc-protein.[8−13] A major advance in this chemoenzymatic method is the discovery of novel endoglycosidase mutants (glycosynthases) that can use highly activated sugar oxazoline as donor substrate for transglycosylation, but lack the activity to hydrolyze the ground state product because of the site-directed mutation at the critical catalytic residue.[11,13,14] Two glycosynthase mutants, the EndoA-N171A and the EndoM-N175A originated from *Arthrobacter protophormiae* and *Mucor hiemalis endo-β-N*-acetylglucosaminidases (Endo-A and Endo-M), respectively, were shown to be particularly useful for synthesizing glycoproteins carrying large natural high-mannose and complex type N-glycans.[11] A key hypothesis in the present synthetic design is that a large synthetic N-glycan oxazoline (**4**) with a lactose moiety attached at the outer mannose residue of the natural high-mannose core could also serve as a donor substrate of the glycosynthase mutant EndoA-N171A or EndoM-N175A for transglycosylation. Thus, the synthesis of glycoprotein targets **1** and **2** could be reduced to the preparation of GlcNAc-RNase (**3**) and the key oligosaccharide oxazoline (**4**) (Figure 2). Retrosynthetic disconnection of **4** led to three major building blocks, the D2D3 arm pentasaccharide fragment (**5**), the lactose-containing D1 arm fragment (**6**), and the core disaccharide glycosyl acceptor (**7**) (Figure 2). The retrosynthetic design of the large N-glycan oxazoline (**4**) was similar to the chemical synthesis of the monoglucosylated N-glycan as reported previously,[6a] which also used a convergent coupling of the D1 and D2D3 building blocks with a core β-mannoside moiety. But different protecting groups and different glycosyl donors and acceptors were used.

Chemical Synthesis of the Selectively Modified and Monoglucosylated High-Mannose Type N-Glycan Oxazoline (4). The synthesis of the target N-glycan oxazoline (**4**) required the preparation of three key building blocks **5**, **6**, and **7**. The preparation of the D2D3 arm pentasaccharide fragment (**5**) was summarized in Scheme 1. Briefly, selective de-O-acetylation of **8** with acetyl chloride in MeOH gave the 2-OH derivative (**9**), which was glycosylated with the known glycosyl imidate **10**[15] to provide disaccharide **11**. Compound **11** was converted into the corresponding glycosyl trichloroacetimidate **12**,[16] which was then used to glycosylate diol **13**[17] under the catalysis of TMSOTf to afford the pentasaccharide derivative (**14**) in 97% yield. De-O-acylation followed by O-benzylation gave the per-O-benzylated thioglycoside (**15**). Finally, the thioglycoside was converted into the glycosyl fluoride (**5**) by treatment with NBS and then with DAST (Scheme 1).

For the synthesis of lactose-containing pentasaccharide intermediate (**6**), the known thioglycoside (**16**)[18] was treated with NBS, followed by DAST, to give a mixture of α- and β-lactosyl fluoride (β/α, 12:1), from which the β-lactosyl fluoride (**17**) was isolated in 88% yield. Glycosylation between **17** and acceptor **18**,[19] via activation with $Cp_2Zr(OTf)_2$ and DTBMP,[20] afforded single α-stereoisomer **19**, which was isolated in 68% yield. A relatively small coupling constant of the H-1 of Glc ($J_{1,2}$ = 3.5 Hz) suggested that the newly formed glycosidic bond between the Glc and Man moieties is in an α-configuration. Compound **19** was then converted into glycosyl fluoride **20**, and the latter was coupled with disaccharide **21** under the promotion of Cp_2HfCl_2/AgOTf to provide pentasaccharide **22** in 69% yield. Changing the benzoyl groups to benzyl groups gave the corresponding thioglycoside (**23**), which was then converted to glycosyl fluoride **6** by NBS-promoted hydrolysis and subsequent treatment of the resulting hemiacetal with DAST (Scheme 2). On the other hand, the core disaccharide (**7**) was prepared following our previously reported procedures.[10]

With the key synthetic building blocks in hand, we next turned our attention to the assembly of the dodecasaccharide oxazoline (**4**). As outlined in Scheme 3, glycosylation of glycosyl fluoride **6** with disaccharide **7** under the promotion of Cp_2HfCl_2/AgOTf gave heptasaccharide **24** as a single isomer in 62% yield. It should be noted that an initial attempt to use thioglycoside **23** directly as

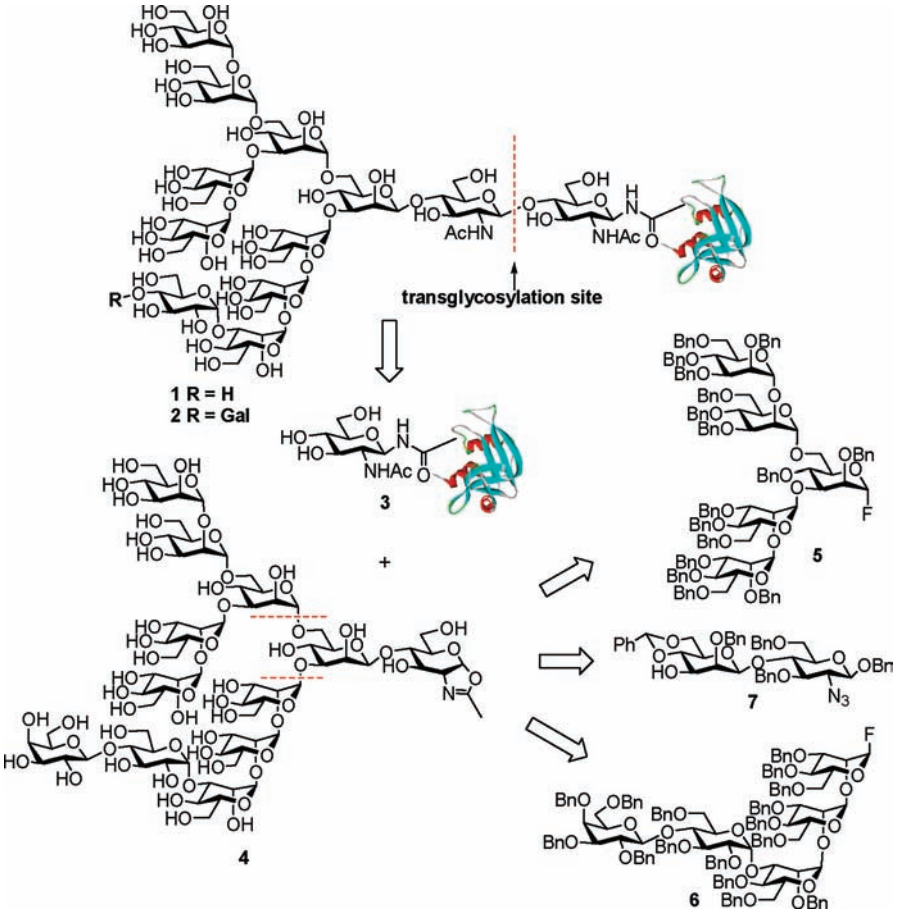

Figure 2. Retrosynthetic analysis of glycoproteins **1** and **2**.

Scheme 1. Synthesis of the D2D3 Arm Pentasaccharide 5[a]

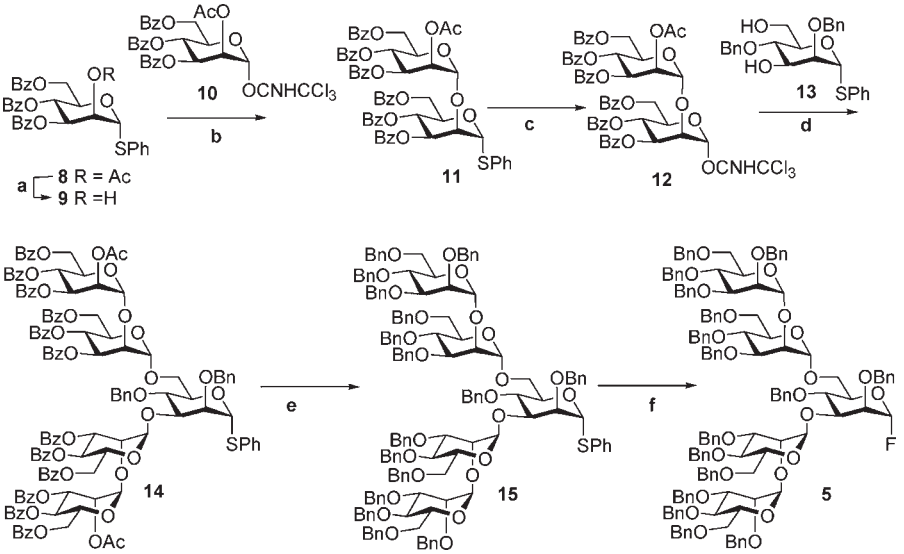

[a] Reagents and yields: (a) 5% AcCl in MeOH, 82%. (b) TMSOTf, 84%. (c) (1) NBS, H_2O, quant.; (2) CCl_3CN, DBU, 86%. (d) TMSOTf, 97%. (e) (1) NaOMe, MeOH; (2) NaH, BnBr, 86%. (f) (1) NBS, H_2O; (2) DAST, 70%.

glycosyl donor for coupling with disaccharide acceptor **7** via the $(BrC_6H_4)_3NSbCl_6$-promoted radical glycosylation[21] gave only a very low yield of corresponding heptasaccharide **24**, even when a large amount of the promoter was applied (data not shown). This was probably due to the low reactivity of thioglycoside **23**. The benzylidene acetal group in **24** was removed by mild acidic

Scheme 2. Synthesis of Pentasaccharide 6[a]

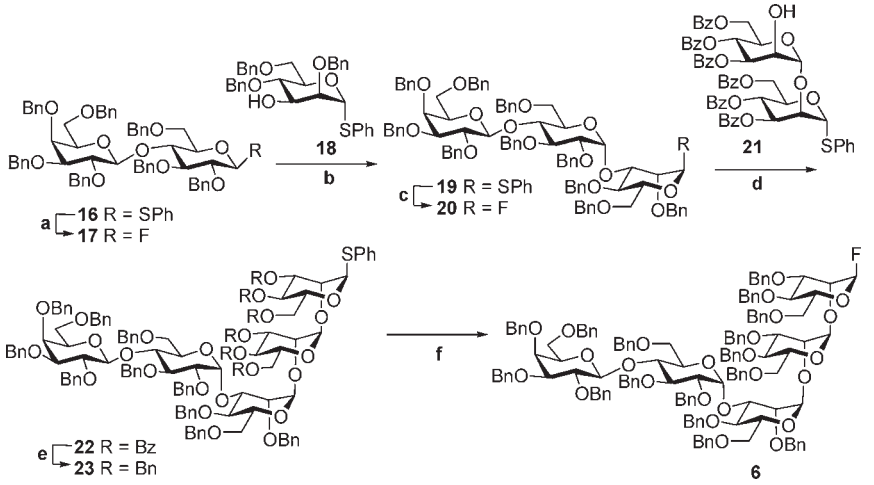

[a] Reagents and yields: (a) (1) NBS, H_2O, quant.; (2) DAST, 88%. (b) $Cp_2Zr(OTf)_2$, DTBMP, 68%. (c) (1) NBS, H_2O, quant.; (2) DAST, 91%. (d) Cp_2HfCl_2, AgOTf, 69%. (e) (1) NaOMe, MeOH; (2) NaH, BnBr, 88% in two steps. (f) (1) NBS, H_2O; (2) DAST, 94% in two steps.

Scheme 3. Synthesis of Dodecasaccharide Oxazoline 4[a]

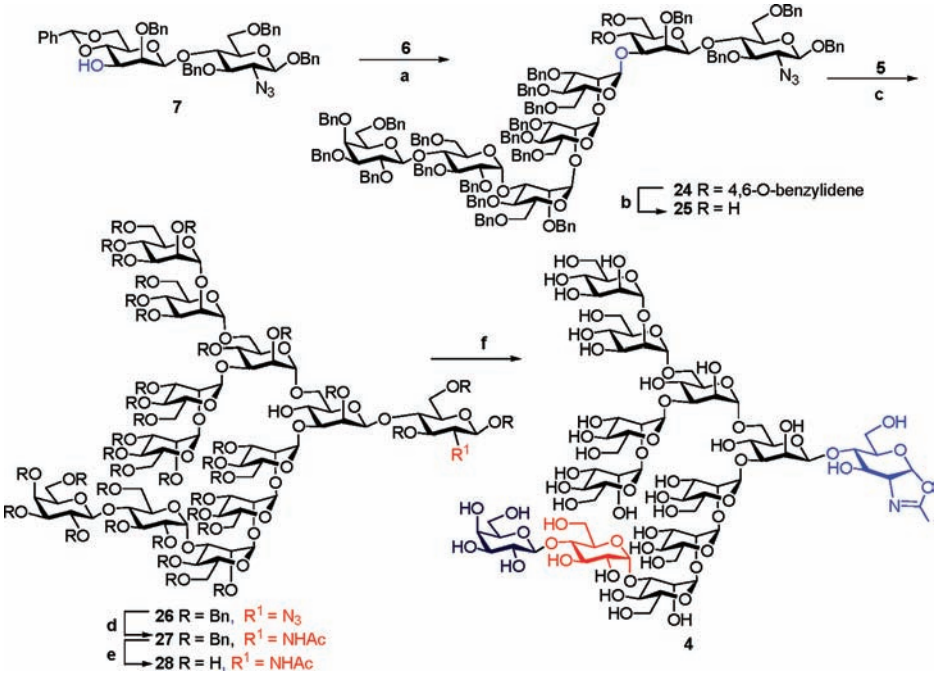

[a] Reagents and yields: (a) Cp_2HfCl_2, AgOTf, 62%. (b) AcOH-EtOH-H_2O, 91%. (c)Cp_2HfCl_2, AgOTf, 61%. (d) AcSH, 2,6-lutidine, 86%. (e) H_2, $Pd(OH)_2/C$, 92%. (f) 2-Chloro-1,3-dimethylimidazolinium chloride (DMC), TEA, quant.

hydrolysis to afford diol **25**, which was then selectively glycosylated at the primary hydroxyl group with pentasaccharide fragment **5** to provide the dodecasaccharide skeleton (**26**) in 61% yield. The α-mannoside linkage for the newly generated glycosidic bond in **26** was evident by the relatively large coupling constants (over 170 Hz) between the C-1 and H-1 of all the α-mannosides (the coupling constants ($^1J_{CH}$) for the 8 α-mannosides and one α-glucoside appeared at 174.7, 174.0, 173.9, 173.8, 173.8, 173.3, 172.3, 171.8, and 170.3 Hz, respectively). Conversion of the 2-azido group into the 2-acetamido group was achieved by treatment with AcSH in the presence of 2,6-lutidine to give **27** in 86% yield. De-O-benzylation was performed via hydrogenolysis of **27** in the presence of $Pd(OH)_2/C$ to afford the free dodecasaccharide **28**. The removal of the multiple O-Bn groups by Pd-catalyzed hydrogenolysis went very well to give the free oligosaccharide (**28**) in almost quantitative yield. Finally, oxazoline formation was achieved in a single step by treatment of free oligosaccharide **28** with an excess amount of 2-chloro-1,3-dimethylimidazolinium chloride (DMC)/TEA[12,22] to furnish the dodecasaccharide oxazoline (**4**), which was isolated by gel filtration in a quantitative yield (Scheme 3).

Scheme 4. Synthesis of Homogeneous Glycoproteins 1, 2, and 30

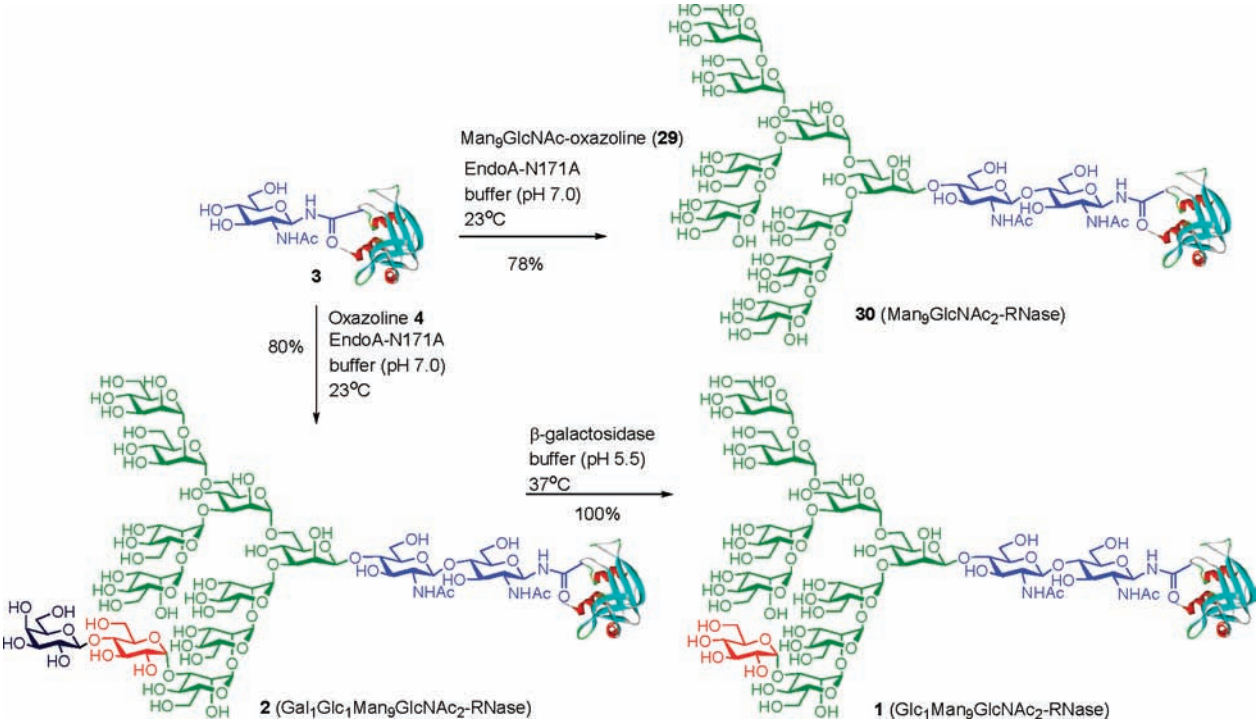

Synthesis of the Target Glycoproteins through Enzymatic Transglycosylation. We have previously shown that a glycosynthase mutant, EndoA-N171A, was able to transfer sugar oxazoline of natural high-mannose type N-glycans to a GlcNAc-protein acceptor to form a homogeneous glycoprotein with the natural β-1,4-linkage for the newly generated glycosidic bond.[11] The use of the glycosynthase mutant is important for the synthesis, as wild-type Endo-A leads to quick hydrolysis of the high-mannose type glycoprotein product. To test whether the lactosemodified high-mannose N-glycan oxazoline (**4**) serves as a donor substrate for the enzyme, we performed the EndoA-N171A catalyzed transglycosylation between oxazoline **4** and GlcNAc-RNase **3** (donor/acceptor, 7:1) in a phosphate buffer (pH 7.0) (Scheme 4). The GlcNAc-RNase was prepared by deglycosylation of natural bovine ribonuclease B (Man_{5-9}-$GlcNAc_2$-RNase) with Endo-H, following our previously reported procedure.[9] We found that the selectively modified high-mannose type N-glycan oxazoline (**4**) acted as a good substrate for EndoA-N171A, and the enzymatic reaction led to a gradual formation of glycoprotein product **2** that appeared slightly earlier than the acceptor GlcNAc-RNase (**3**) under a reverse-phase HPLC condition (for an HPLC monitoring profile of the enzymatic transglycosylation, see Figure S1, Supporting Information). After 5 h, the reaction was stopped and the product (**2**) was readily isolated by HPLC in 80% yield (calculated on the basis of the used GlcNAc-RNase). The transformation of GlcNAc-RNase (**3**) to the product could be driven to completion when additional sugar oxazoline was added to the reaction mixture. The enzymatic reaction was readily performed on a milligram scale of the GlcNAc-protein acceptor, but could be scaled up when needed. Moreover, upon the completion of the enzymatic reaction, we were able to efficiently recover the excess sugar oxazoline by HPLC in the form of free reducing oligosaccharide, which was recycled for the transglycosylation by conversion into the activated sugar oxazoline (**4**), using a single-step transformation in water with 2-chloro-1,3-dimethylimidazolinium chloride (DMC)/TEA.[12,22] The homogeneity of the product $Gal_1Glc_1Man_9GlcNAc_2$-RNase (**2**) was evident from its SDS−PAGE and ESI−MS analysis (Figure 3). Moreover, Dionex HPAEC-PAD monosaccharide composition analysis of **2** gave the expected molar ratios of monosaccharides: Gal/Glc/Man/GlcN = 1:1:9:2 (Figure S2, Supporting Information). To obtain the monoglucosylated glycoform (**1**), the synthetic glycoprotein (**2**) was treated with a β-galactosidase from *Streptococcus pneumoniae* in a phosphate buffer (pH 5.5). It was found that the *Streptococcus* β-galactosidase could selectively and efficiently remove the terminal galactose to give the monoglucosylated glycoform $Glc_1Man_9GlcNAc_2$-RNase (**1**) in essentially quantitative yield, without any side reactions. The SDS−PAGE and ESI−MS analysis of glycoproteins **1** and **2** were shown in Figure 3. The purified Gal_1Glc_1-$Man_9GlcNAc_2$-RNase (**2**) (lane 3, Figure 3A) and $Glc_1Man_9GlcNAc_2$-RNase (**1**) (lane 4, Figure 3A) appeared as a single band at ca. 16 kDa, which is about 2 kDa larger than the precursor GlcNAc-RB (**3**) that had an apparent molecular weight of 14 kDa (lane 2, Figure 3A). The data indicates the attachment of a single large N-glycan to the precursor after transglycosylation. Deconvolution of the MS data of glycoprotein **2** gave a molecular mass of 15 872 Da, which matched well with the calculated molecular mass (M = 15 870 Da). On the other hand, deconvolution of the ESI−MS data of glycoprotein **1** gave a molecular mass of 15 710 Da, which was in good agreement with the calculated molecular mass (M = 15 708 Da). For comparison, we also prepared the nonglucosylated glycoform, $Man_9GlcNAc_2$-RNase (**30**), using $Man_9GlcNAc$-oxazoline **29**[11] as the donor substrate. The EndoA-N171A catalyzed reaction gave a 78% yield of glycoprotein **30** under the same conditions as that for the synthesis of glycoprotein **2**. The transglycosylation yield for the synthesis of

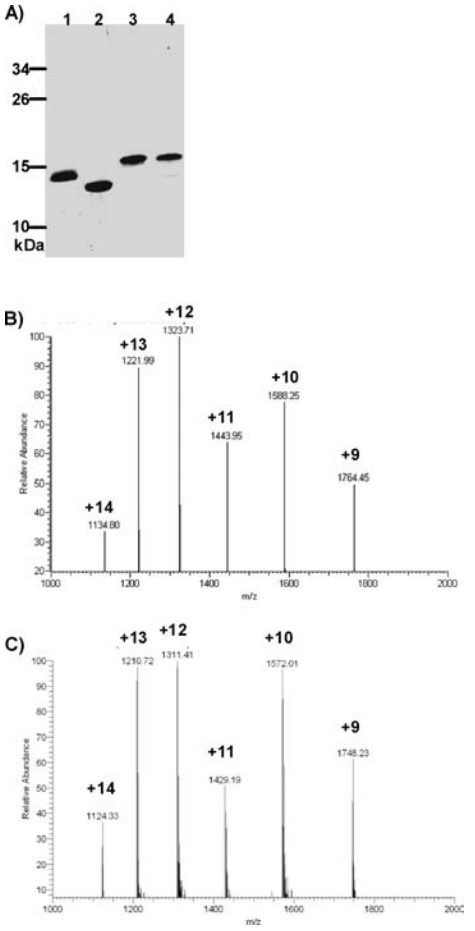

Figure 3. Analysis of the synthetic glycoproteins. (A) SDS−PAGE: lane 1, natural RNase B; lane 2, GlcNAc-RNase; lane 3, glycoprotein **2**; lane 4, glycoprotein **1**. (B) ESI−MS of glycoprotein **2**. (C) ESI−MS of glycoprotein **1**.

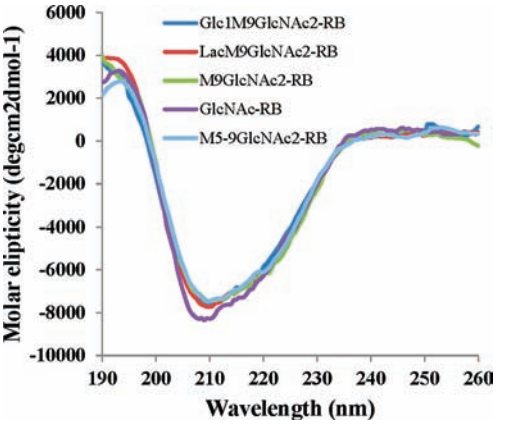

Figure 4. The CD spectra of different glycoforms of ribonuclease. GN-RB, the GlcNAc-RB; LacM9GN2-RB, $Gal_1Glc_1Man_9GlcNAc_2$-RB; M9GN2-RB, $Man_9GlcNAc_2$-RB; GlcM9GN2-RB, $Glc_1Man_9GlcNAc_2$-RB; M5−9GN2-RB, $Man_{5-9}GlcNAc_2$-RB (the natural bovine RNase B). Except the extensively trimmed glycoform GlcNAc-RB, all other synthetic glycoforms that bear a large N-glycan as well as the natural RNase B showed very similar CD spectroscopic profiles.

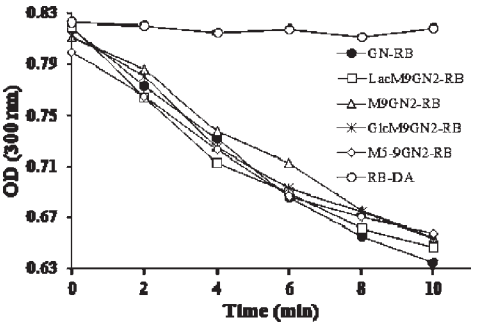

Figure 5. RNA-hydrolyzing activity of different glycoforms of ribonuclease B (RB). A solution of yeast RNA (0.5 mg/mL) was incubated with each of the RNase glycoforms (4 μg/mL) in a buffer (pH 5.0), and the UV absorbance (300 nm) of the solution was recorded. This figure shows a representative profile of the RNA hydrolysis by the individual glycoforms of RNase B (RB). RB-DA stands for the heat-deactivated natural RNase B.

glycoproteins **2** and **30** was comparable, suggesting that the glycosynthase mutant EndoA-N171A was equally efficient for transferring the sugar oxazolines corresponding to both the natural high-mannose type N-glycan and its derivatives with selective modifications on the outer residues of the high-mannose core.

Circular Dichroism and RNA-Hydrolyzing Activity of the Synthetic RNase Glycoforms. To evaluate the structural integrity of the synthetic glycoproteins, we measured their circular dichroism (CD) spectra and compared them to the natural RNase B (**31**) that carries heterogeneous high-mannose type N-glycans ($Man_{5-9}GlcNAc_2$). The CD spectroscopic analysis was performed in the far UV wavelength region (190−260 nm) that allows the monitoring of the changes in secondary structures of the glycoproteins. As shown in Figure 4, all the synthetic glycoforms with a large synthetic high-mannose type N-glycan, including glycoforms **1**, **2**, and **30**, had almost identical spectroscopic profiles similar to that of the natural RNase B. An analysis using the web-based DICHROWEB server[23] gave essentially the same estimate (within the error) on the percentages of secondary structures for glycoforms **1**, **2**, and **30**, as well as the natural RNase B (**31**): 21 ± 8.8% α-helix, 33 ± 7.5% β-strands, 13 ± 1.8% β-turns, and 33 ± 0.9% unordered structures. In comparison, the truncated form GlcNAc-RNase (**3**), in which the N-glycan was removed to leave only the innermost GlcNAc residue at the N-glycosylation site, seemed to have an enhanced α-helical content. The estimated percentages of the secondary structures for the GlcNAc-RNase (**3**) were 31 ± 9.9% α-helix, 27 ± 4.5% β-strands, 12 ± 2.0% β-turns, and 30 ± 5.6% unordered structures. The CD spectroscopy of GlcNAc-RNase (**3**) was very similar to that of the glycan-truncated RNase B carrying heterogeneous $Man_{2-4}GlcNAc_2$ glycans as reported previously.[24] These results suggest that the chemoenzymatic manipulations including the enzymatic deglycosylation of RNase B and subsequent enzymatic transglycosylation with sugar oxazoline did not denature the glycoproteins. In addition, the experimental data also indicate that as long as the high-mannose core was retained, modification at the outer residues of the N-glycan had less impact on the protein's conformations.

To probe the functions of the synthetic glycoforms, we measured the enzymatic activity of the respective synthetic glycoforms as well as the natural RNase B (Sigma). RNase B is

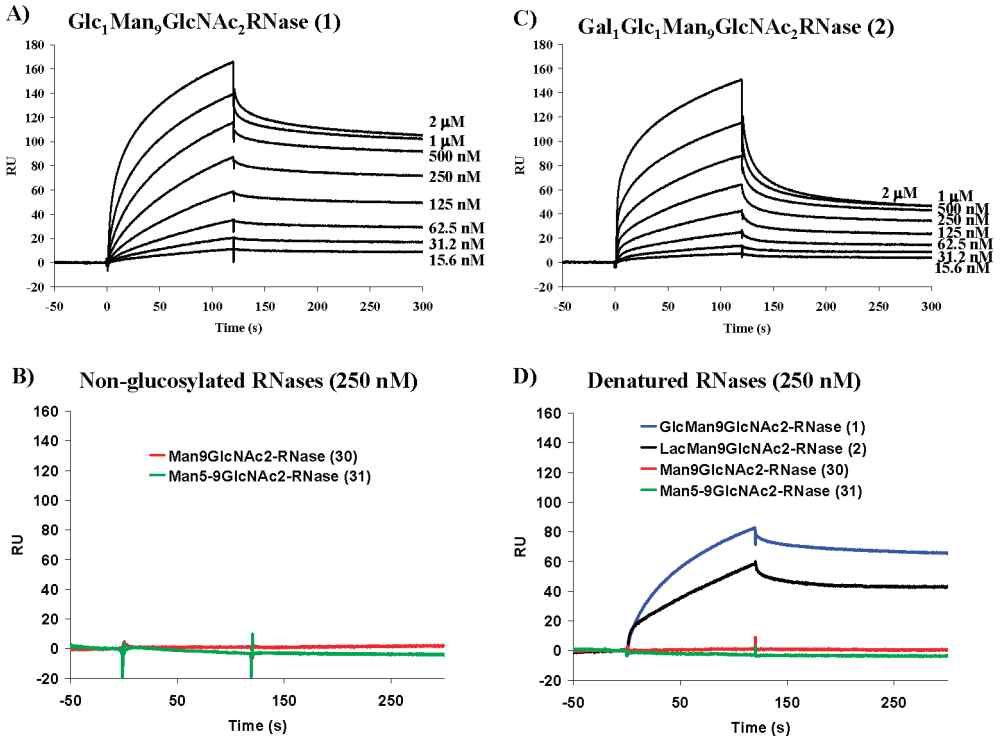

Figure 6. SPR sensorgrams of the binding between immobilized lectin CRT and different RNase glycoforms. The binding analysis was performed at 10 °C, (A) with $Glc_1Man_9GlcNAc_2$-RNase (**1**), (B) with nonglucosylated $Man_9GlcNAc_2$-RNase (**30**) and natural $Man_{5-9}GlcNAc_2$-RNase (**31**), (C) with $Gal_1Glc_1Man_9GlcNAc_2$-RNase (**2**), (D) with denatured RNase glycoproteins.

known to catalyze the hydrolysis of the 3′,5′-phosphodiester bonds of RNA. It was previously reported that degradation of RNA by ribonuclease was accompanied by a shift in the UV absorbance of the RNA substrate toward the shorter wavelengths.[25] Thus, measurement of the decrease of absorbance at 300 nm constitutes a simple and very straightforward method for assessing the RNA-hydrolyzing activity of RNase.[25] Using a commercially available yeast RNA extract as the substrate for testing hydrolytic activity, we measured the enzymatic hydrolysis of the yeast RNA by the individual RNase glycoforms. A representative enzymatic hydrolysis profile was shown in Figure 5. We found that the synthetic glycoforms (**1**, **2**, and **30**) that carry a large N-glycan had similar enzymatic activity as that of the natural RNase B, while the glycoform (GlcNAc-RB) that carries only a monosaccharide moiety at the glycosylation site showed a slightly higher enzymatic activity than the others. Dwek and co-workers previously performed a comparative study on the hydrolytic activity of RNase A (nonglycosylated form) with several truncated glycoforms of RNase B, including the $Man_5GlcNAc_2$, $Man_1GlcNAc_2$, and $GlcNAc_2$-glycoforms.[26] Their studies indicated that the attachment of an N-glycan at Asn-34 in the bovine ribonuclease resulted in 2- to 4-fold decrease in the enzymatic activity when compared with the nonglycosylated RNase A. The difference in enzymatic activity between the nonglycosylated and glycosylated RNases (RNase A and B, respectively) was mainly attributed to steric hindrance exerted by the attachment of a large N-glycan. They also found that natural RNase B that contains a mixture of $Man_{5-9}GlcNAc_2$ glycoforms had the same activity as that of $Man_5GlcNAc_2$-RNase B, suggesting that attachment of additional residues beyond the high-mannose core did not further affect the enzymatic activity. Our experimental data with the synthetic glycoforms are consistent with the previously reported observations. Together with the CD analysis, our RNA-hydrolyzing activity data provides strong evidence indicating that the RNase glycoforms synthesized through our chemoenzymatic approach are properly folded and are fully functional with almost identical enzymatic activity as the natural RNase B.

Binding Studies with Lectin Calreticulin (CRT). With the successful synthesis of the glycan-defined RNase glycoforms, we performed binding studies with the molecular chaperone calreticulin (CRT) using surface plasmon resonance (SPR) technology. The lectin CRT was immobilized on the chips and the different glycoforms were probed as analytes at 10 °C. The results are shown in Figure 6. As expected, the synthetic $Glc_1Man_9GlcNAc_2$-RNase (**1**) was efficiently recognized by the immobilized CRT (Figure 6A), with a deduced K_D of 38 nM at 10 °C ($k_{on} = 1.28 \times 10^4\ M^{-1}\ s^{-1}$; $k_{off} = 4.82 \times 10^{-4}\ s^{-1}$). In contrast, the nonglucosylated $Man_9GlcNAc_2$-RNase (**30**), as well as the native RNase B ($Man_{5-9}GlcNAc_2$-RNase) (**31**), did not show any binding to CRT within the tested concentration range (30−2000 nM) (Figure 6B). These results confirm the essential role of the α-1,3-linked glucose moiety in the $Glc_1Man_9GlcNAc_2$ glycan for CRT recognition.

The SPR analysis of the interaction between CRT and the selectively modified glycoform (**2**) yielded an interesting result (Figure 6C). We found that CRT showed significant affinity to the $Gal_1Glc_1Man_9GlcNAc_2$-RNase (**2**), in which the terminal glucose was masked by a β-1,4-linked galactose. Fitting the binding data to a 1:1 Langmuir binding model gave a K_D of 110 nM for the interaction ($k_{on} = 1.81 \times 10^4\ M^{-1}\ s^{-1}$; $k_{off} = 1.99 \times 10^{-3}\ s^{-1}$). A comparison of the K_D values indicates that $Glc_1Man_9GlcNAc_2$-RNase (**1**) binds to CRT about 2-fold more efficiently than $Gal_1Glc_1Man_9GlcNAc_2$-RNase (**2**) binds to

CRT. The kinetic data suggests that this was attributed mainly to the relatively fast dissociation rate (k_{off}) of the modified monoglucosylated derivative. Nevertheless, the high affinity of glycoform **2** to lectin CRT (with a K_D of 110 nM) indicated that selective attachment of a galactose moiety at the 4-OH of the terminal Glc residue did not significantly impair the interaction between the monoglucosylated glycan and lectin CRT.

The high-affinity binding of the monoglucosylated high-mannose type glycoproteins (**1** and **2**), together with the observation that the corresponding nonglucosylated $Man_9GlcNAc_2$-RNase (**30**) and natural $Man_{5-9}GlcNAc_2$-RNase (**31**) did not bind to CRT, clearly indicated the requirement of the specific α-1,3-glucose moiety for CRT recognition. To further confirm that the binding of $Glc_1Man_9GlcNAc_2$-RNase (**1**) and $Gal_1Glc_1Man_9GlcNAc_2$-RNase (**2**) to CRT was not caused by potential changes of conformations in the protein domains, we denatured the natural RNase B (**31**) and the synthetic RNase glycoproteins (**1**, **2**, and **30**). Partial and complete denaturations were achieved by dissolving the glycoproteins in a Tris buffer (pH 8.6) containing 8 M urea, in the absence or presence of 0.15 M dithiothreitol (DTT) (reducing agent), respectively, following the previously reported methods.[27] Reverse-phase HPLC (RP-HPLC) analysis indicated that while the folded glycoprotein appeared as a single peak, partial denaturation of RNase B led to the formation of a new species that appeared as a broad peak with a longer retention time as compared with the folded glycoprotein (Figure S3, Supporting Information), suggesting the exposure of some hydrophobic residues in the denatured species. On the other hand, complete denaturation with the cleavage of the disulfide bonds led to a major peak that appeared with a longer retention time than the native species, together with a series of minor species (Figure S3). The synthetic glycoproteins demonstrated similar RP-HPLC patterns as the RNase B before and after denaturation (data not shown). We performed the CRT binding studies with the completely denatured glycoproteins (Figure 6D). It was found that the denatured monoglucosylated glycoproteins (**1** and **2**) showed almost the same CRT-binding patterns as the corresponding folded glycoproteins (**1** and **2**), respectively. On the other hand, the nonglucosylated glycoproteins, $Man_9GlcNAc_2$-RNase (**30**) and $Man_{5-9}GlcNAc_2$-RNase (**31**), still did not bind to CRT after denaturation. The partially denatured glycoproteins behaved the same as the corresponding completely denatured glycoprotein in CRT-binding (data not shown). Taken together, our binding studies with well-defined homogeneous RNase glycoforms that are in either folded or denatured states clearly suggest that CRT recognizes specifically the monoglucosylated high-mannose type N-glycan in the RNase, independent of the protein domain and its folding states. These results are consistent with previous observations when mixtures of monoglycosylated and nonglycosylated RNase B glycoforms were used for CRT recognition studies.[3,28] It should be pointed out that there were different views on whether CRT and calnexin (CNX) have direct interactions with the protein domain in protein folding process. Some studies suggested that the monoglucosylated oligosaccharides are necessary and sufficient for association of a glycoprotein with CRT and CNX, regardless of its folding status;[3,28] other studies indicated that in addition to its lectin property to recognize monoglucosylated oligosaccharides, CRT could also bind to unfolded nonglycosylated protein domain to form stable complexes that prevent protein aggregation, although folded protein domain did not bind to CRT.[29] In the latter case, it was also observed that the binding of CRT to unfolded polypeptide was substrate dependent, as the affinity of CRT to unfolded proteins was relatively weak compared with its binding to monoglucosylated glycoprotein and the affinity varied with different proteins. Thus, an explanation for the lack of CRT binding to unfolded nonglucosylated RNase B was that unfolded RNase B might lack the polypeptide elements recognized by CRT.[29] It should be also pointed out that while lectin CRT (and CNX) may or may not have direct interactions with the misfolded or unfolded protein domain of a given glycoprotein, the lectins, upon binding with the monoglucosylated glycoform of the misfolded protein, are able to recruit other molecular chaperones such as the disulfide isomerase-like protein ERp57 that directly recognizes and binds to misfolded protein domain to promote appropriate folding of the glycoprotein. With the availability of the homogeneous, monoglucosylated glycoforms of RNase B and other glycoproteins, now we have the molecular probes to address how CRT-mediated recognition acts in concert with chaperone ERp57 for promoting protein folding.

Some kinetic studies on the binding of CRT with monoglucosylated oligosaccharide substrates were previously reported.[4,5,7,30] The binding studies with synthetic Glc_1Man_{1-4} oligosaccharides indicated that the whole D1 arm of $Glc_1Man_9GlcNAc_2$ was involved in CRT recognition.[5,7,30] For example, an isothermal titration calorimetry (ITC) measurement indicated that the synthetic tetrasaccharide Glcα1−3Manα1−2Manα1−2Manα1-Me was at least 50-fold more potent than the disaccharide Glcα1−3Manα1-Me in binding to CRT.[5] A SPR binding study using monoglucosylated chicken IgG fractions as the model glycoproteins for CRT binding at 10 °C gave a k_1 and k_{-1} of 1.5×10^4 M^{-1} s^{-1} and 2×10^{-2} s^{-1}, respectively.[4] The CRT binding kinetic parameters for $Glc_1Man_9GlcNAc_2$ were very similar to the monoglucosylated chicken IgG fractions under the same binding conditions.[4] In comparison, our $Glc_1Man_9GlcNAc_2$-RNase/CRT binding study gave comparable association rates ($k_{on} = 1.28 \times 10^4$ M^{-1} s^{-1}). However, our dissociation rate with $Glc_1Man_9GlcNAc_2$-RNase ($k_{off} = 4.82 \times 10^{-4}$ s^{-1}) seemed much lower than that reported for the monoglucosylated IgG fractions. It is not clear whether this was due to the difference of the protein context (IgG vs RNase) that may affect the conformations of the N-glycans differentially or due to the heterogeneous glycosylation nature of the IgG molecules used. A more detailed binding study using well-characterized homogeneous monoglucosylated IgG and other glycoproteins would be required to clarify this point.

The relatively high affinity of $Gal_1Glc_1Man_9GlcNAc_2$-RNase (**2**) to lectin CRT (with a K_D of 110 nM) suggests that the 4-OH of the terminal Glc residue could tolerate modification without significantly impairing its interaction with lectin CRT. Recently, the crystal structure of CRT complexed with Glc_1Man_3 tetrasaccharide was solved at a 1.95 Å resolution.[31] The structure of the complex clearly shows that the Glc_1Man_3 tetrasaccharide binds to a long channel on CRT involving an extensive network of hydrogen bonds and hydrophobic interactions. The 2-OH of Glc was involved in hydrogen bonding with Gly124 and Lys111 of CRT; the 3-OH of Glc was engaged with the Tyr128 of CRT, while the 4-OH of Glc was protruding toward outside the cavity without any hydrogen bonds involved (Figure S4, Supporting Information). This structural arrangement suggests that the 4-OH may tolerate some modifications and has a space to accommodate a substituent. On the other hand, the 3-OH is involved in a hydrogen-bond network with residue Tyr128 of CRT. The X-ray crystal structure of the complexes also explains why CRT does not bind to the natural diglucosylated ($Glc_2Man_9GlcNAc_2$)

intermediate glycoform, in which the second Glc residue was α-1,3-linked to the innermost Glc residue.[1,2] Our findings suggest that the 4-OH position of the monoglucosylated ligands would be suitable for selective modification with appropriate tags to provide novel probes for structural or functional studies.

■ CONCLUSION

An efficient chemoenzymatic synthesis of homogeneous glycoprotein probes, including the monoglucosylated glycoform $Glc_1Man_9GlcNAc_2$-RNase and its selectively modified derivative, was achieved. The relaxed substrate specificity of the endoglycosidase mutant and the highly convergent nature of the chemoenzymatic method point to a potentially general approach to the assembly of both natural and tailor-made glycoprotein probes that are hitherto difficult to obtain for CRT/CNX-mediated protein folding studies. The synthetic homogeneous RNase glycoforms showed very similar global structures and RNA-hydrolyzing activities. The binding studies with lectin CRT indicated the essential role of the monoglucose residue in the glycoprotein for CRT recognition, and the unexpected high affinity of the selectively modified monoglucosylated glycoform implicated interesting structural features in the molecular recognition of CRT. The availability of the well-defined glycoprotein probes should enable a more detailed mechanistic study on how a fine N-glycan structure functions in concert with a misfolded or partially folded protein domain to provide the right signal in the protein quality control process. Among others, an immediate application of the synthetic monoglucosylated glycoform is to probe the mechanism and kinetics of the CRT/CNX-mediated interactions between a misfolded glycoprotein and other molecular chaperones such as the disulfide isomerase-like protein ERp57. The synthetic monoglucosylated RNase glycoform ($Glc_1Man_9GlcNAc_2$-RNase) can be intentionally denatured and misfolded. Then, the complex of misfolded $Glc_1Man_9GlcNAc_2$-RNase and lectin CRT (or CNX) can be used to decipher how differentially misfolded status of the complex recruits and interacts with the disulfide isomerase-like protein ERp57 for proper protein folding.

■ EXPERIMENTAL SECTION

Materials and Methods. The N171A mutant of *endo-β-N*-acetylglucosaminidase from *A. protophormiae* (Endo-A) was overproduced in *Escherichia coli* following the reported procedure.[11] Calreticulin (CRT) was purchased from United States Biological (Swampscott, MA). Bovine pancreatic ribonuclease B was purchased from Sigma-Aldrich (St. Louis, MO). Thin-layer chromatography (TLC) was performed on silica gel coated aluminum plates (Sigma-Aldrich). Flash column chromatography was performed on silica gel 60 (230−400 mesh). SDS−PAGE was performed on a gradient (4−10%) polyacrylamide gel. NMR spectra were recorded on a VARIAN 500 MHz spectrometer and JEOL ECX 400 MHz spectrometer. The chemical shifts were assigned in parts per million (ppm). TMS and acetone were used as internal standards for solvents $CDCl_3$ and D_2O, respectively. ESI−MS spectra were measured on a Micromass ZQ-4000 single-quadrupole mass spectrometer and LXQ linear ion trap mass spectrometer (Thermo Scientific). High-resolution (HR) MALDI-TOF spectra were measured on a MALDI-TOF/TOF 4800 spectrometer (Applied Biosystems) with 2,5-dihydroxybenzoic acid as matrix and Cal 4700 standard peptide mixture was used (Applied Biosystems) as internal standard. Analytical RP-HPLC for glycoprotein analysis was performed on a Waters 626 HPLC instrument with a C18 column (3.5 μm, 4.6 × 250 mm) at 40 °C. The column was eluted with a linear gradient of 24−33% aq MeCN containing 0.1% TFA for 30 min at a flow rate of 0.5 mL/min. Preparative HPLC was performed with a Waters 600 HPLC instrument on a Waters C18 column (5.0 μm, 10 × 250 mm). The column was eluted with a gradient of 23−29% aq MeCN containing 0.1%TFA for 30 min at a flow rate of 4 mL/min.

Synthesis of 2,3,4,6-Tetra-*O*-benzyl-β-D-galactopyranosyl-(1→4)-3,4,6-tri-*O*-benzyl-β-D-glucopyranosyl Fluoride (17). To an ice-cooled solution of phenyl 2,3,4,6-tetra-*O*-benzyl-β-D-galactopyranosyl)-(1→4)-2,3,6-tri-*O*-benzyl-1-thio-β-D-glucopyranoside **16** (913 mg, 0.857 mmol) in acetone−water (9:1, 10 mL) was added NBS (458 mg, 2.57 mmol). The reaction mixture was stirred for 1 h. Monitoring of the reaction with TLC (hexane−ethyl acetate, 2/1) indicated complete hydrolysis of thioglycoside. The reaction was quenched with $NaHCO_3$ and the mixture was extracted with ethyl acetate. The extract was dried and concentrated to dryness. The dried crude product was dissolved in anhydrous CH_2Cl_2 (18 mL) and the solution was cooled to −20 °C. To the solution was added DAST (225 μL, 1.71 mmol). The reaction mixture was stirred for 1 h and then quenched with saturated $NaHCO_3$ (aq). The mixture was washed with brine, dried over Na_2SO_4, and filtered. The filtrate was concentrated and the residue was subjected to silica gel chromatography (hexane−ethyl acetate, 2/1) to give the β-lactosyl fluoride (**17**) (736 mg, 88%) and its α-isomer (68 mg, 8%). Characterization of the β-lactosyl fluoride (**17**): HRMS MALDI-TOF: $[M + Na]^+$ calcd for $C_{61}H_{63}O_{10}FNa$, 997.4303, found 997.4303. ^1H NMR ($CDCl_3$, 500 MHz): δ 7.34−7.12 (m, 35H), 5.22 (dd, *J* = 53.5, 6.5 Hz, H-1, 1H), 4.99 (d, *J* = 11.0 Hz, PhCH_2, 1H), 4.96 (d, *J* = 12.0 Hz, PhCH_2, 1H), 4.80 (d, *J* = 11.5 Hz, PhCH_2, 1H), 4.78 (d, *J* = 13.0 Hz, PhCH_2, 1H), 4.73−4.68 (m, 5H), 4.55 (d, *J* = 11.5 Hz, PhCH_2, 1H), 4.54 (d, *J* = 12.0 Hz, PhCH_2, 1H), 4.40 (d, *J* = 7.5 Hz, H-1^{gal}, 1H), 4.39 (d, *J* = 12.5 Hz, PhCH_2, 1H), 4.34 (d, *J* = 12.0 Hz, PhCH_2, 1H), 4.25 (d, *J* = 11.5 Hz, PhCH_2, 1H), 4.04 (br t, *J* = 9.0 Hz, 1H), 3.90 (d, *J* = 2.4 Hz, H-4^{gal}, 1H), 3.81 (dd, *J* = 10.5, 4.0 Hz, 1H), 3.74 (dd, *J* = 10.0, 7.5 Hz, 1H), 3.64 (dd, *J* = 9.5, 1.0 Hz, 1H), 3.59−3.50 (m, 3H), 3.47 (dd, *J* = 9.0, 2.0 Hz, 1H), 3.39−3.32 (m, 3H); ^{13}C NMR ($CDCl_3$, 100 MHz): δ 139.13, 138.92, 138.86, 138.61, 138.19, 138.16, 138.07, 128.51, 128.45, 128.38, 128.30, 128.18, 128.01, 127.96, 127.88, 127.71, 127.57, 109.78, 102.78, 82.62, 81.82, 81.72, 81.07, 80.85, 80.03, 75.91, 75.46, 75.22, 75.15, 74.85, 74.69, 73.70, 73.56, 73.37, 73.19, 72.71, 68.24, 67.93. Characterization of the α-lactosyl fluoride: HRMS MALDI-TOF: $[M + Na]^+$ calcd for $C_{61}H_{63}O_{10}FNa$, 997.4303, found 997.4364. ^1H NMR ($CDCl_3$, 500 MHz): δ 7.36−7.12 (m, 35H), 5.48 (dd, *J* = 53.5, 2.4 Hz, H-1, 1H), 5.07 (d, *J* = 11.0 Hz, PhCH_2, 1H), 4.97 (d, *J* = 11.0 Hz, PhCH_2, 1H), 4.83 (d, *J* = 12.0 Hz, PhCH_2, 1H), 4.80 (d, *J* = 11.0 Hz, PhCH_2, 1H), 4.74−4.70 (m, 5H), 4.66 (d, *J* = 12.0 Hz, PhCH_2, 1H), 4.56 (d, *J* = 11.0 Hz, PhCH_2, 1H), 4.51(d, *J* = 12.0 Hz, PhCH_2, 1H),, 4.38 (d, *J* = 12.0 Hz, PhCH_2, 1H), 4.33 (d, *J* = 7.0 Hz, H-1^{gal}, 1H), 4.31 (d, *J* = 12.0 Hz, PhCH_2, 1H), 4.25 (d, *J* = 12.0 Hz, PhCH_2, 1H), 4.01 (br t, *J* = 9.0 Hz, 1H), 3.90−3.88 (m, 2H), 3.86−3.80 (m, 2H), 3.75 (dd, *J* = 10.0, 8.0 Hz, 1H), 3.57−3.48 (m, 2H), 3.45 (dd, *J* = 9.0, 2.0 Hz, 1H), 3.39−3.32 (m, 3H); ^{13}C NMR ($CDCl_3$, 125 MHz): δ 139.03, 138.72, 138.69, 138.52, 138.49, 138.33, 138.00, 137.85, 128.37, 128.22, 127.98, 127.89, 127.79, 127.72, 127.66, 127.55, 127.52, 127.40, 127.17, 105.83, 102.77, 82.46, 79.88, 79.67, 78.24, 75.59, 75.50, 75.33, 74.73, 73.88, 73.71, 734.43, 73.16, 72.60, 68.21, 67.27.

Synthesis of Phenyl 2,3,4,6-Tetra-*O*-benzyl-β-D-galactopyranosyl-(1→4)-2,3,6-tri-*O*-benzyl-α-glucopyranosyl-(1→3)-2,4,6-tri-*O*-benzyl-1-thio-α-D-mannopyranoside (19). A mixture of monosaccharide **18** (38 mg, 0.070 mmol), glycosyl fluoride **17** (82 mg, 0.084 mmol), and MS 4A (0.50 g) in toluene−tetrahydrofuran (9/1, 18 mL) was stirred for 30 min and cooled to −20 °C. Then, DTBMP (22 mg, 0.105 mmol) and $Cp_2Zr(OTf)_2$ (46 mg, 0.77 mmol) were added. The resulting mixture was stirred for 5 h under argon at −20 °C to room temperature and then filtered through a Celite pad. The filtrate was diluted

with EtOAc and washed with saturated $NaHCO_3$ (aq), water, and brine, dried over Na_2SO_4, and filtered. The filtrate was concentrated to dryness. The residue was subjected to flash chromatography on silica gel (hexane−ethyl acetate, 4/1) to give trisaccharide **19** (72 mg, 68%). ESI−MS: calcd for $C_{94}H_{96}O_{15}S$, M = 1497.82; Found (m/z), 1520.43 $[M + Na]^+$. ^1H NMR ($CDCl_3$, 500 MHz): δ 7.46−7.43 (m, 2H), 7.33−7.09 (m, 53H), 5.54 (s, H-1, Man, 1H), 5.12 (d, J = 4.0 Hz, H-1^{Glc},1H), 5.04 (d, J = 11.0 Hz, PhCH_2, 1H), 4.94 (d, J = 11.0 Hz, PhCH_2, 1H), 4.72 (d, J = 10.5 Hz, PhCH_2, 1H), 4.69 (d, J = 12.5 Hz, PhCH_2, 1H), 4.67 (d, J = 13.0 Hz, PhCH_2, 1H), 4.64 (d, J = 11.5 Hz, PhCH_2, 1H), 4.62 (d, J = 12.5 Hz, PhCH_2, 1H), 4.58−4.48 (m, 10H), 4.43 (d, J = 12.0 Hz, PhCH_2, 1H), 4.37−4.30 (m, 4H), 4.20 (d, J = 12.5 Hz, PhCH_2, 1H), 4.16 (br s, 1H), 4.05 (dd, J = 9.0, 2.0 Hz, 1H), 4.02−3.97 (m, 2H), 3.88 (m, 2H), 3.81−3.76 (m, 2H), 3.70 (m, 2H), 3.63 (dd, J = 11.5, 2.0 Hz, 1H) 3.49−3.45 (m, 2H), 3.35−3.32 (m, 3H); ^{13}C NMR ($CDCl_3$, 100 MHz): δ 139.57, 139.16, 138.83, 138.55, 138.32, 138.19, 134.74, 131.60, 129.03, 128.39, 128.29, 128.22, 128.04, 127.98, 127.87, 127.81, 127.65, 127.51, 127.27, 127.15, 127.01, 103.31, 99.73, 85.28, 82.65, 80.08, 79.87, 78.88, 77.52, 75.31, 75.07, 74.74, 73.70, 73.49, 73.38, 73.26, 73.02, 72.62, 71.55, 69.36, 68.56, 68.34.

Synthesis of 2,3,4,6-Tetra-*O*-benzyl-β-D-galactopyranosyl-(1→4)-2,3,6-tri-*O*-benzyl-α-D-glucopyranosyl-(1→3)-2,4,6-tri-*O*-benzyl-α-D-mannopyranosyl Fluoride (20). To an ice-cold solution of compound **19** (203 mg, 0.135 mmol) in acetone−water (9:1, 6 mL) was added NBS (72 mg, 0.406 mmol) and the mixture was stirred for 2 h. TLC (hexane−ethyl acetate, 2/1) indicated complete disappearance of starting materials. The mixture was diluted with EtOAc. The organic layer was washed with saturated $NaHCO_3$ (aq), water, and brine; dried over Na_2SO_4; and filtered. The filtrate was concentrated to dryness to give the hemiacetal (ESI−MS, calculated, M = 1405.65; found (m/z), 1428.46 $[M + Na]^+$). The crude product was dissolved in anhydrous CH_2Cl_2 (10 mL) and cooled to −10 °C. To the solution was added DAST (45 μL, 0.34 mmol). The mixture was stirred for 50 min at −10 °C and the reaction was then quenched with saturated $NaHCO_3$ (aq). The organic layer was separated and washed with water and brine, dried over Na_2SO_4, and filtered. The filtrate was concentrated and the residue was subjected to flash chromatography on silica gel (toluene−ethyl acetate, 12/1) to give compound **20** (173 mg, 91%). HRMS MALDI-TOF: $[M + Na]^+$ calcd for $C_{88}H_{91}O_{15}FNa$, 1429.6239, found 1429.6284. ^1H NMR ($CDCl_3$, 500 MHz): δ 7.32−7.08 (m, 50H), 5.48 (d, J_{H-F} = 55.0 Hz, H-1, 1H), 5.15 (d, J = 4.0 Hz, H-1^{Glc},1H), 5.04 (d, J = 11.0 Hz, PhCH_2, 1H), 5.01 (d, J = 12.0 Hz, PhCH_2, 1H), 4.95 (d, J = 11.5 Hz, PhCH_2, 1H), 4.72−4.62 (m, 7H), 4.58−4.52 (m, 3H), 4.47 (d, J = 7.5 Hz, H-1^{Gal}, overlapped, 1H), 4.48−4.44 (m, 3H, overlapped with H-1^{Gal}), 4.36−4.31 (m, 3H), 4.21 (d, J = 12.5 Hz, PhCH_2, 1H), 4.08−4.05 (m, 2H), 4.02−3.96 (m, 3H), 3.92−3.85 (m, 3H), 3.78 (dd, J = 11.0, 4.0 Hz, 1H), 3.71 (br t, J = 9.0 Hz, 1H), 3.68−3.62 (m, 3H), 3.50−3.46 (m, 2H), 3.36−3.34 (m, 3H); ^{13}C NMR ($CDCl_3$, 125 MHz): δ 139.34, 139.03, 138.72, 138.46, 138.17, 138.07, 138.06, 128.37, 128.32, 128.15, 127.97, 127.88, 127.78, 127.68, 127.61, 127.43, 127.36, 127.27, 127.21,126.95, 105.79 (d, J = 229.0 Hz, C-1), 103.26, 99.36, 82.49, 79.99, 79.85, 78.65, 77.46, 75.20, 75.00, 74.66, 74.32, 73.85, 73.62, 73.39, 73.32, 73.18, 72.91, 72.54, 71.48, 68.70, 68.49, 68.25.

Synthesis of Phenyl 3,4,6-Tri-*O*-benzoyl-α-D-mannopyranosyl-(1→2)-3,4,6-tri-*O*-benzoyl-1-thio-α-D-mannopyranoside (21). To a solution of compound **11** (498 mg, 0.452 mmol) in CH_2Cl_2 (12 mL) was added 5% AcCl in MeOH (15 mL) at 0 °C and the resulting mixture was stirred for 8 h. The solution was concentrated to dryness and the residue was subjected to flash silica gel column chromatography (toluene−EtOAc, 15/1) to afford compound **21** (374 mg, 79%) as a white amorphous solid. HRMS MALDI-TOF: $[M + Na]^+$ calcd for $C_{60}H_{50}O_{16}SNa$, 1081.2717, found 1081.2711. ^1H NMR ($CDCl_3$, 500 MHz): δ 8.04−7.91 (m, 12H), 7.52−7.15 (m, 23H), 6.00 (dd, J = 10.0, 9.5 Hz, H-4, 1H), 5.94 (dd, J = 10.0, 9.5 Hz, H-4′, 1H), 5.87 (s, H-1, 1H), 5.83 (dd, J = 10.0, 3.0 Hz, H-3, 1H), 5.78 (dd, J = 10.0, 3.0 Hz, H-3′, 1H), 5.21 (s, H-1′, 1H), 4.95 (m, H-5, 1H), 4.70 (br s, H-2, 1H), 4.60 (m, H-6, 2H), 4.53 (m, H-5′, 1H), 4.50−4.26 (m, H-2′, H-6′, 3H); ^{13}C NMR ($CDCl_3$, 125 MHz): δ 166.24 (PhCO × 2), 165.61 (PhCO × 2), 165.52 (PhCO), 165.41 (PhCO), 133.47, 133.41, 133.37, 133.03, 131.86, 129.90, 129.72, 129.28, 128.96, 128.42, 127.94, 101.41, 86.63, 72.17, 71.69, 69.88, 67.55, 66.87, 63.66, 63.38.

Synthesis of Phenyl 2,3,4,6-Tetra-*O*-benzyl-β-D-galactopyranosyl-(1→4)-2,3,6-tri-*O*-benzyl-α-D-glucopyranosyl-(1→3)-2,4,6-tri-*O*-benzyl-α-D-mannopyranosyl-(1→2)-3,4,6-tri-*O*-benzoyl-α-D-mannopyranosyl-(1→2)-3,4,6-tri-*O*-benzoyl-1-thio-α-D-mannopyranoside (22). To a mixture of glycosyl fluoride **20** (1.15 g, 0.817 mmol), disaccharide **21** (0.72 g, 0.681 mmol), and dried MS (2.30 g, 4 Å) in CH_2Cl_2 (30 mL) were added Cp_2HfCl_2 (0.46 g, 1.23 mmol) and AgOTf (0.63 g, 2.451 mmol) at 0 °C. The reaction mixture was stirred for 4 h at room temperature and then filtered through a Celite pad. The filtrate was washed with saturated $NaHCO_3$ (aq), water, and brine; dried over Na_2SO_4; and filtered. The solution was concentrated to dryness. The residue was subjected to flash chromatography on silica gel (toluene−ethyl acetate, 15/1) to afford **22** (1.15 g, 69%). ESI−MS: calcd for $C_{148}H_{140}O_{31}S$, M = 2446.74; Found (m/z), 2469.51 $[M + Na]^+$. ^1H NMR ($CDCl_3$, 500 MHz): δ 7.96−7.91 (m, Ar), 7.51−6.99 (m, Ar), 6.03 (t, 1H), 5.96 (dd, J = 10.0, 9.5 Hz, 1H), 5.91 (s, 1H), 5.85 (dd, J = 9.5, 3.0 Hz, 1H) 5.77 (dd, 1H), 5.50 (br s, 1H), 5.01−4.92 (m, H-1^{Glc}, H-1^{Man}, PhCH_2, overlapped, 5H), 4.67−4.50 (m, 13H), 4.42−4.32 (m, 8H), 4.24−4.19 (m, 3H), 4.13−4.02 (m, 4H), 3.89−3.84 (m, 6H), 3.76−3.62 (m, 3H), 3.48−3.46 (m, 3H), 3.33−3.32 (m, 4H). ^{13}C NMR ($CDCl_3$, 125 MHz): δ 166.22 (PhCO), 166.19 (PhCO), 165.69 (PhCO), 165.43 (PhCO), 165.33 (PhCO), 165.29 (PhCO), 139.49, 139.09, 18.71, 138.49, 1138.26, 138.03, 133.31, 132.93, 132.75, 131.53, 130.00, 129.92, 129.73, 129.59, 129.20, 129.02, 128.55, 128.34, 128.27, 128.13, 127.98, 127.84, 127.78, 127.70, 127.64, 127.43, 127.30, 127.15, 126.85, 102.91, 100.62, 100.51, 98.86, 86.39, 82.61, 79.91, 79.49, 78.97, 78.23, 75.98, 75.20, 74.77, 74.64, 73.66, 73.38, 73.09, 72.80, 72.53, 71.98, 71.48, 71.00, 69.82, 68.25, 67.89, 67.02, 63.74, 63.57.

Synthesis of Phenyl 2,3,4,6-Tetra-*O*-benzyl-β-D-galactopyranosyl-(1→4)-2,3,6-tri-*O*-benzyl-α-D-glucopyranosyl-(1→3)-2,4,6-tri-*O*-benzyl-α-D-mannopyranosyl-(1→2)-3,4,6-tri-*O*-benzyl-α-D-mannopyranosyl-(1→2)-3,4,6-tri-*O*-benzyl-1-thio-α-D-mannopyranoside (23). To a solution of compound **22** (1.21 g, 0.493 mmol) in toluene−methanol (1/1, 20 mL) was added a solution of NaOMe in MeOH (0.5 M, 0.5 mL). The mixture was stirred for 5 h at 50 °C when TLC and ESI−MS indicated the completion de-O-acylation. Solvent was removed and the residual foam was dissolved in anhydrous DMF (10 mL) and cooled to 0 °C. To the solution were added NaH (177 mg, 7.39 mmol), BnBr (0.88 mL, 7.39 mmol), and TBAI (34 mg, 0.09 mmol). The reaction mixture was stirred for 26 h at room tmeperature, diluted with EtOAc, and washed with water and brine. The organic layer was dried over Na_2SO_4, filtered, and the filtrate was concentrated. The residue was subjected to flash chromatography on silica gel (toluene−ethyl acetate, 14/1) to give **23** as a foam (1.03 g, 88%). HRMS MALDI-TOF: $[M + Na]^+$ calcd for $C_{148}H_{152}O_{25}SNa$, 2384.0241, found 2384.0249. ^1H NMR ($CDCl_3$, 500 MHz): δ 7.42−7.01 (m, Ar, 85H), 5.73 (s, H-1, 1H), 5.24 (s, H-1, 1H), 5,12 (s, H-1, 1H), 5.70 (d, J = 3.0 Hz, H-1^{Glc}, 1H) 4.99 (d, J = 10.5 Hz, PhCH_2, 1H), 4.92 (d, J = 12.0 Hz, PhCH_2, 1H), 4.84 (d, J = 11.0 Hz, PhCH_2, 1H), 4.78 (d, J = 10.5 Hz, PhCH_2, 1H), 4.67 (d, J = 11.0 Hz, PhCH_2, 1H), 4.63 (d, J = 12.0 Hz, PhCH_2, 1H), 4.62−4.54 (m, 6H), 4.52−4.43 (m, H-1^{Gal} overlapped, 16H), 4.33−4.25 (m, 6H), 4.19 (d, J = 11.5 Hz, 1H), 4.13−4.08 (m, 4H), 3.98−3.79 (m, 11H), 3.75 (dd, J = 10.0, 9.5 Hz, 1H), 3.71−3.53 (m, 4H), 3.49−3.44 (m, 2H), 3.34−3.29 (m, 4H).

Synthesis of 2,3,4,6-Tetra-*O*-benzyl-β-D-galactopyranosyl-(1→4)-2,3,6-tri-*O*-benzyl-α-D-glucopyranosyl-(1→3)-2,4,6-

tri-*O*-benzyl-α-D-mannopyranosyl-(1→2)-3,4,6-tri-*O*-benzyl-α-D-mannopyranosyl-(1→2)-3,4,6-tri-*O*-benzyl-α-D-mannopyranosyl Fluoride (6). To a solution of compound **23** (0.969 g, 0.41 mmol) in acetone (10 mL) were added NBS (0.183 g, 1.04 mmol) and H_2O (0.5 mL) at −10 °C. The reaction mixture was stirred for 2 h, when TLC (toluene−EtOAc, 6/1) revealed the disappearance of starting material. The solvent was evaporated and residue was dissolved in EtOAc. The solution was successively washed with saturated $NaHCO_3$ (aq), water, and brine; dried over Na_2SO_4; and filtered. The filtrate was concentrated. The residue was dissolved in anhydrous CH_2Cl_2 (15 mL). To the solution was added DAST (108 μL, 0.83 mmol) at −10 °C. The mixture was stirred for 45 min, diluted with CH_2Cl_2, and washed with saturated $NaHCO_3$ (aq), brine, and water. The organic layer was dried over Na_2SO_4 and filtered. The filtrate was concentrated and the residue was subjected to flash chromatography on silica gel (toluene−EtOAc, 15/1) to afford compound **6** (0.898 g, 93%). HRMS MALDI-TOF: $[M + Na]^+$ calcd for $C_{142}H_{147}FO_{25}Na$, 2294.0113, found 2294.0135. ^1H NMR ($CDCl_3$, 500 MHz): δ 7.70−7.13 (m, Ar, 80H), 5.73 (d, *J* = 54.5 Hz, H-1, 1H), 5.24 (s, H-1, 1H), 5,09 (br s, H-1, H-1^{Glc} overlapped, 2H), 5.00 (d, *J* = 10.5 Hz, PhC*H*$_2$, 1H), 4.92 (d, *J* = 11.5 Hz, PhC*H*$_2$, 1H), 4.82 (d, *J* = 10.5 Hz, PhC*H*$_2$, 1H), 4.80 (d, *J* = 11.5 Hz, PhC*H*$_2$, 1H), 4.68 (d, *J* = 11.0 Hz, PhC*H*$_2$, 1H), 4.63 (d, *J* = 12.0 Hz, PhC*H*$_2$, 1H), 4.62−4.54 (m, 6H), 4.51−4.39 (m, H-1^{Gal}, overlapped, 17H), 4.35−4.26 (m, 5H), 4.23−4.19 (m, 3H), 4.13−4.08 (m, 3H), 3.97−3.91 (m, 5H), 3.84−3.79 (m, 5H), 3.77−3.66 (m, 4H), 3.60−3.54 (m, 3H), 3.50−3.47 (m, 2H), 3.33−3.29 (m, 4H). ^{13}C NMR ($CDCl_3$, 125 MHz): δ 139.50, 139.10, 138.79, 138.60, 138.54, 138.48, 138.36, 138.33, 138.28, 138.27, 138.24, 138.13, 137.95, 132.46, 130.88, 128.51, 128.35, 128.32, 128.30, 128.29, 128.19, 128.14, 128.06, 128.03, 127.97, 127.90, 127.87, 127.85, 127.78, 127.74, 127.71, 127.66, 127.63, 127.60, 127.56. 127.49, 127.45, 127.42, 127.31, 127.22, 127.19, 126.88, 126.75, 106.62, 102.99, 101.19, 99.38, 90.03, 82.60, 79.99, 79.58, 79.07, 78.17, 75.25, 75.15, 75.00, 74.85, 74.64, 73.97, 73.80, 73.61, 73.38, 73.32, 73.28, 73.24, 73.11, 72.52, 72.46, 72.35, 71.99, 71.66, 71.23, 69.22, 68.65, 68.24, 68.17.

Synthesis of Benzyl 2,3,4,6-Tetra-*O*-benzyl-β-D-galactopyranosyl-(1→4)-2,3,6-tri-*O*-benzyl-α-D-glucopyranosyl-(1→3)-2,4,6-tri-*O*-benzyl-α-D-mannopyranosyl-(1→2)-3,4,6-tri-*O*-benzyl-α-D-mannopyranosyl-(1→2)-3,4,6-tri-*O*-benzyl-α-D-mannopyranosyl-(1→3)-2-*O*-benzyl-4,6-*O*-benzylidene-β-D-mannopyranosyl-(1→4)-2-azido-3,6-di-*O*-benzyl-2-deoxy-β-D-glucopyranoside (24). To a mixture of pentasaccharide donor **6** (870 mg, 0.382 mmol), disaccharide acceptor **7** (223 mg, 0.273 mmol), and dried MS (1 g, 4 Å) in CH_2Cl_2 (20 mL) were added Cp_2HfCl_2 (232 mg, 0.612 mmol) and AgOTf (315 mg, 1.225 mmol) at 0 °C. The mixture was stirred for 5 h at room temperature. After dilution with CH_2Cl_2, the reaction mixture was filtered through a Celite pad. The filtrate was washed with saturated $NaHCO_3$ (aq), brine, and water; dried over Na_2SO_4; and filtered. The filtrate was concentrated to dryness and the residue was subjected to flash chromatography on silica gel (toluene−EtOAc, 6/1) to give compound **24** (517 mg, 62%). MALDI-TOF MS: calcd for $C_{189}H_{195}O_{35}N_3$, M = 3068.57; Found (*m*/*z*), 3091.56 $[M + Na]^+$. ^1H NMR ($CDCl_3$, 500 MHz): δ 7.38−7.08 (m, 105H), 5.34 [s, PhC*H*(O)$_2$, 1H], 5.29 (s, H-1, 1H), 5.24 (s, H-1, 1H), 5.12 (d, H-1^{Glc}, overlapped, 1H), 5.07 (s, H-1, 1H), 5.11−5.03 (m, PhC*H*$_2$, overlapped, 2H), 4.99 (d, *J* = 10.5 Hz, PhC*H*$_2$, 1H), 4.93−4.89 (m, 3H), 4.84−4.82 (m, 3H), 4.73 (br s, 2H), 4.69−4.53 (m, 9H), 4.51−4.40 (m, 12H), 4.36−4.16 (m, 10H), 4.13−4.06 (m, 3H), 3.98−3.95 (m, 3H), 3.93−3.85 (m, 4H), 3.80−3.77 (m, 3H), 3.73−3.67 (m, 4H), 3.62−3.45 (m, 5H), 3.43−3.29 (m, 5H), 3.15 (dd, 1H), 2.87 (m, 1H); ^{13}C NMR ($CDCl_3$, 100 MHz): δ 139.46, 139.07, 138.76, 138.73, 138.61, 138.58, 138.40, 138.49, 138.46, 138.40, 138.35, 138.25, 138.15, 138.02, 137.68, 137.17, 136.80, 129.00, 128.96, 128.50, 128.4 128.35, 128.31, 128.27, 128.24, 128.14, 128.10, 128.05, 127.99, 127.93, 127.91, 127.87, 127.83, 127.76, 127.74, 127.68, 127.65, 127.59, 127.52, 127.48, 127.46, 127.41, 127.38, 127.26, 127.19, 127.16, 127.14, 126.85, 126.70, 102.92, 101.09, 101.07, 100.33, 100.03, 82.56, 81.54, 79.98, 79.71, 79.55, 79.13, 78.79, 78.21, 75.54, 75.39, 75.22, 75.13, 75.07, 74.91, 74.82, 74.60, 73.71, 73.60, 73.41, 73.35, 73.28, 73.13, 73.07, 72.90, 72.74, 72.49, 72.35, 72.26, 71.55, 71.46, 71.25, 70.74, 69.72, 69.57, 68.98, 68.31, 68.22, 68.07, 66.99, 65.69.

Synthesis of Benzyl 2,3,4,6-Tetra-*O*-benzyl-β-D-galactopyranosyl-(1→4)-2,3,6-tri-*O*-benzyl-α-D-glucopyranosyl-(1→3)-2,4,6-tri-*O*-benzyl-α-D-mannopyranosyl-(1→2)-3,4,6-tri-*O*-benzyl-α-D-mannopyranosyl-(1→2)-3,4,6-tri-*O*-benzyl-α-D-mannopyranosyl-(1→3)-2-*O*-benzyl-β-D-mannopyranosyl-(1→4)-2-azido-3,6-di-*O*-benzyl-2-deoxy-β-D-glucopyranoside (25). A solution of compound **24** (320 mg, 0.104 mmol) in AcOH−EtOH−H_2O (4/1/1) was stirred at 100 °C for 5 h. The reaction mixture was then concentrated to dryness and the residue was subjected directly to flash chromatography on silica gel (hexane−EtOAc, 2/1) to afford compound **25** (284 mg, 91%) as a white foam. HRMS MALDI-TOF: $[M + Na]^+$ calcd for $C_{182}H_{191}N_3O_{35}Na$, 3001.3156, found 3001.3189. ^1H NMR ($CDCl_3$, 500 MHz): δ 7.39−7.08 (m, 100H), 5.31 (s, H-1, 1H), 5.30 (s, H-1, 1H), 5.17 (s, H-1, 1H), 5.10 (d, PhC*H*$_2$, overlapped, 1H), 5.08 (d, H-1^{Glc} overlapped, 1H), 5.00 (d, *J* = 11.0 Hz, PhC*H*$_2$, 1H), 4.99 (d, *J* = 11.0 Hz, PhC*H*$_2$, 1H), 4.92 (d, *J* = 11.5 Hz, PhC*H*$_2$, 1H), 4.90 (d, *J* = 11.0 Hz, PhC*H*$_2$, 1H), 4.81 (d, *J* = 10.5 Hz, PhC*H*$_2$, 1H), 4.80 (d, *J* = 11.5 Hz, PhC*H*$_2$, 1H), 4.70−4.39 (m, 25H), 4.34−4.24 (m, 6H), 4.19 (d, *J* = 11.5 Hz, 2H), 4.11−4.07 (m, 3H), 3.96−3.91 (m, 3H), 3.85−3.73 (m, 5H), 3.70−3.60 (m, 5H), 3.58−3.51 (m, 4H), 3.49−3.43 (m, 4H), 3.41−3.27 (m, 4H), 3.21 (br d, 1H), 3.11 (m, 1H), 2.84 (m, 1H); ^{13}C NMR ($CDCl_3$, 125 MHz): δ 139.49, 139.18, 139.10 138.98, 138.79, 138.57, 138.45, 138.35, 138.25, 138.03, 137.98, 137.65, 137.52, 136.84, 128.53, 128.45, 128.35, 128.25, 128.12, 128.00, 127.94, 127.85, 127.76, 127.72, 127.68, 127.66, 127.63, 127.61, 127.58, 127.63, 127.61, 127.58, 127.54, 127.51, 127.47, 127.43, 127.37, 127.35, 127.32, 127.21, 127.09, 127.04,126.78, 102.97, 100.84, 100.31, 100.22, 99.56, 82.59, 81.39, 80.30, 79.99, 79.56, 79.10, 78.20, 75.75, 75.55, 75.38, 75.15, 74.97, 74.82, 74.69, 74.58, 74.09, 73.75, 73.48, 73.36, 73.08, 72.62, 72.49, 72.38, 71.85, 71.46, 71.36, 70.73, 70.16, 69.65, 69.01, 68.24, 68.11, 65.82, 62.44.

Synthesis of Benzyl 2,3,4,6-Tetra-*O*-benzyl-β-D-galactopyranosyl-(1→4)-2,3,6-tri-*O*-benzyl-α-D-glucopyranosyl-(1→3)-2,4,6-tri-*O*-benzyl-α-D-mannopyranosyl-(1→2)-3,4,6-tri-*O*-benzyl-α-D-mannopyranosyl-(1→2)-3,4,6-tri-*O*-benzyl-α-D-mannopyranosyl-(1→3)-{2,3,4,6-tetra-*O*-benzyl-α-D-mannopyranosyl-(1→2)-3,4,6-tri-*O*-benzyl-α-D-mannopyranosyl-(1→3)-[2,3,4,6-tetra-*O*-benzyl-α-D-mannopyranosyl-(1→2)-3,4,6-tri-*O*-benzyl-α-D-mannopyranosyl-(1→6)]-2,4-di-*O*-benzyl-α-D-mannopyranosyl-(1→6)}-2-*O*-benzyl-β-D-mannopyranosyl-(1→4)-2-azido-3,6-di-*O*-benzyl-2-deoxy-β-D-glucopyranoside (26). To a mixture of pentasaccharide donor **5** (139 mg, 0.061 mmol), heptasaccharide acceptor **25** (181 mg, 0.061 mmol), and dried MS (1 g, 4 Å) in CH_2Cl_2 (10 mL) was added Cp_2HfCl_2 (369 mg, 0.971 mmol) and AgOTf (499 mg, 1.94 mmol) at 0 °C. The mixture was stirred for 9 h at room temperature and then diluted with CH_2Cl_2, and filtered through a Celite pad. The filtrate was washed with saturated $NaHCO_3$ (aq), brine, and water; dried over Na_2SO_4; and filtered. The solution was concentrated and the residue was subjected to flash chromatography on silica gel (hexane−EtOAc, 2/1) to obtain compound **26** (193 mg, 61%). MALDI-TOF MS: calcd for $C_{324}H_{337}O_{60}N_3$, M = 5233.13; Found (*m*/*z*), 5256.12 $[M + Na]^+$. ^1H NMR ($CDCl_3$, 500 MHz): δ 7.43−6.92 (m, 180H), 5.31 (s, H-1, 1H), 5.28 (s, H-1, 2H), 5.20 (s, H-1, 1H), 5.17 (s, H-1, 2H), 5.09 (br s, 2H), 4.99 (m, 2H), 4.93 and 4.91 (2s, overlapped, 2H), 4.85−4.68 (m, 7H), 4.70−4.28 (m, 67H), 4.24−4.17 (m, 4H), 4.15−4.02 (m, 9H), 3.99−3.77 (m, 25H), 3.73−3.57 (m, 9H), 3.53−3.40 (m, 12H),

3.35−3.29 (m, 6H), 3.23−3.04 (m, 7H); ^{13}C NMR ($CDCl_3$, 125 MHz): δ 139.51−137.98 (Ar), 128.68−126.59 (Ar), 102.97, 102.32, 100.95, 100.30, 99.52, 99.35, 98.90, 96.76, 96.73, 82.61, 81.25, 80.25, 80.10, 79.98, 79.56, 79.45, 79.35, 78.13, 78.07, 75.54, 75.26, 75.23, 75.16, 74.98, 74.75, 74.71, 74.46, 74.13, 73.95, 73.57, 73.38, 73.19, 73.08, 72.69, 72.49, 72.28, 72.18, 72.01, 71.95, 71.75, 71.51, 70.55, 70.33, 69.40, 69.34, 68.92, 68.52, 68.41, 68.23, 67.62, 66.84, 66.62, 66.52, 65.61.

Synthesis of Benzyl 2,3,4,6-Tetra-*O*-benzyl-β-D-galactopyranosyl-(1→4)-2,3,6-tri-*O*-benzyl-α-D-glucopyranosyl-(1→3)-2,4,6-tri-*O*-benzyl-α-D-mannopyranosyl-(1→2)-3,4,6-tri-*O*-benzyl-α-D-mannopyranosyl-(1→2)-3,4,6-tri-*O*-benzyl-α-D-mannopyranosyl-(1→3)-{2,3,4,6-tetra-*O*-benzyl-α-D-mannopyranosyl-(1→2)-3,4,6-tri-*O*-benzyl-α-D-mannopyranosyl-(1→3)-[2,3,4,6-tetra-*O*-benzyl-α-D-mannopyranosyl-(1→2)-3,4,6-tri-*O*-benzyl-α-D-mannopyranosyl-(1→6)]-2,4-di-*O*-benzyl-α-D-mannopyranosyl-(1→6)}-2-*O*-benzyl-β-D-mannopyranosyl-(1→4)-2-acetamido-3,6-di-*O*-benzyl-2-deoxy-β-D-glucopyranoside (27). To a solution of compound **26** (59.0 mg, 11.27 mmol) in AcSH (3 mL) was added 2,6-lutidine (3 mL) and the solution was stirred at room temperature for 15 h. The reaction mixture was diluted with CH_2Cl_2; washed with saturated $NaHCO_3$ (aq), brine, and water; dried over Na_2SO_4 and filtered. The filtrate was concentrated and the residue was subjected to flash chromatography on silica gel (hexane−EtOAc, 2/1) to give compound **27** (47 mg, 86%) MALDI-TOF MS: calcd for $C_{326}H_{341}O_{61}N$, M = 5249.16; Found (*m*/*z*), 5272.15 $[M + Na]^+$. ^{1}H NMR ($CDCl_3$, 500 MHz): δ 7.39−6.98 (m, 180H), 6.09 (d, *J* = 6.5 Hz, AcN*H*, 1H), 5.32 (s, H-1, 1H), 5.28 (s, H-1, H), 5.20 (s, H-1, 1H), 5.17 (s, H-1, 2H), 5.09 (br s, 2H), 4.99 (m, 2H), 4.93 and 4.91 (2s, overlapped, 2H), 4.85−4.80 (m, 7H), 4.71−4.28 (m, 67H), 4.24−4.18 (m, 4H), 4.15−4.02 (m, 9H), 3.99−3.74 (m, 25H), 3.73−3.57 (m, 9H), 3.55−3.40 (m, 12H), 3.35−3.30 (m, 6H), 3.23−3.04 (m, 7H), 1.71 (s, C*H*$_3$CONH). ^{13}C NMR ($CDCl_3$, 125 MHz): δ 170.25 (*C*O), 139.49−137.56 (Ar), 128.69−126.47 (Ar), 102.99, 100.86, 100.54, 100.22, 100.10, 99.45, 99.16, 96.81, 96.63, 94.76, 82.60, 80.00, 79.92, 79.87, 79.73, 79.57, 79.41, 79.28, 79.04, 78.19, 78.06, 75.39, 75.25, 75.12, 74.80, 74.62, 74.41, 74.01, 73.81, 73.59, 73.38, 73.26, 73.09, 72.94, 72.78, 72.51, 72.24, 72.00, 71.96, 71.67, 71.39, 71.22, 70.64, 70.36, 69.26, 68.98, 68.90, 68.81, 68.63, 68.25, 68.19, 67.53, 66.68, 23.09 (*C*H$_3$CONH).

Synthesis of β-D-Galactopyranosyl-(1→4)-α-D-glucopyranosyl-(1→3)-α-D-mannopyranosyl -(1→2)-α-D-mannopyranosyl-(1→2)-α-D-mannopyranosyl-(1→3)-{α-D-mannopyranosyl-(1→2)-α-D-mannopyranosyl-(1→3)-[α-D-mannopyranosyl-(1→2)-α-D-mannopyranosyl-(1→6)]-α-D-mannopyranosyl-(1→6)}-β-D-mannopyranosyl-(1→4)-2-acetamido-2-deoxy-α,β-D-glucopyranose (28). A mixture of compound **27** (62 mg, 11.8 μmol) and 20% $Pd(OH)_2$/C (41 mg) in 50% AcOH (aq.) (12 mL) was stirred under H_2 atmosphere for 21 h. The reaction mixture was filtered through a Celite pad. The filtrate was dissolved in water and lyophilized. The crude product was purified on a Sephadex LH-20 column by elution with H_2O. Fractions containing the product were pooled and lyophilized to give the free dodecasaccharide (**28**) (22 mg, 92%) as a white solid. MALDI-TOF MS: calcd for $C_{74}H_{125}O_{61}N$, M = 2004.75; Found (*m*/*z*), 2027.67 $[M + Na]^+$, ESI−MS: 1002.84 $[M + 2H]^{2+}$. ^{1}H NMR (D_2O, 500 MHz): δ 5.40 (s, 1H), 5.34 (s, 1H), 5.30 (s, 1H), 5.25 (d, *J* = 2.5 Hz, H-1^{Glc}, 1H), 5.23 (s, H-1, 1H), 5.14 (s, H-1, H), 5.05 (s, H-1, 1H), 5.04 (s, H-1, 2H), 5.09 (br s, 2H), 4.86, 4.76, 4.70 (overlapped with solvent H-OD) 4.45 (d, *J* = 8.0 Hz, H-1^{Gal}, 1H), 4.23−3.53 (m, 72H), 2.04 (s, 3H). ^{13}C NMR (D_2O,, selected signals, 125 MHz): δ 170.21, 101.87, 101.30, 101.06, 99.88, 99.69, 99.21, 99.14, 97.22, 22.98.

Synthesis of 2-Methyl-[β-D-galactopyranosyl-(1→4)-α-D-glucopyranosyl-(1→3)-α-D-mannopyranosyl-(1→2)-α-D-mannopyranosyl-(1→2)-α-D-mannopyranosyl-(1→3)-{α-D-mannopyranosyl-(1→2)-α-D-mannopyranosyl-(1→3)-[α-D-mannopyranosyl-(1→2)-α-D-mannopyranosyl-(1→6)]-α-D-mannopyranosyl-(1→6)}-β-D-mannopyranosyl-(1→4)-1,2-dideoxy-D-glucopyrano]-[2,1-*d*]-2-oxazoline (4). To a solution of compound **28** (4.0 mg, 1.99 nmol) in H_2O (0.5 mL) was added Et_3N (25 μL, 180 nmol) and 2-chloro-1,3-dimethylimidazolinium chloride (DMC) (11 mg, 65 nmol) at 0 °C. The reaction mixture was monitored by DIONEX HPAEC-PAD. Within 1 h, the HPAEC analysis indicated that the free oligosaccharide was converted into a new oligosaccharide that was eluted earlier than the reducing sugar under the HPAEC conditions. The product was purified by gel filtration on a Sephadex G-10 column that was eluted with 0.1% aq TEA to afford sugar oxazoline **4** (4.0 mg, quant.) as a white solid after lyophilization. MALDI-TOF MS: calcd for $C_{74}H_{123}O_{60}N$, M = 1986.73; Found (*m*/*z*), 2009.66 $[M + Na]^+$. ^{1}H NMR (D_2O, 500 MHz): δ 6.09 (d, *J* = 6.5 Hz, H-1, Oxazoline, 1H), 5.37 (s, 1H), 5.32 (s, 1H), 5.29 (s, 1H), 5.25 (d, *J* = 2.5 Hz, H-1^{Glc}, 1H), 5.14 (s, H-1, 1H), 5.03 (s, H-1, 3H), 5.09 (s, H-1, 1H), 4.91 (s, H-1, 1H), 4.44 (d, *J* = 7.5 Hz, H-1^{Gal}, 1H), 4.23−3.54 (m, 69H), 3.07−3.03 (m, 3H), 1.90 (s, 3H). ^{13}C NMR (D_2O, selected signals, 125 MHz): δ 167.8, 102.20, 101.61, 101.06, 99.85, 99.83, 99.11, 97.17, 16.75.

Synthesis of Glycoprotein $Gal_1Glc_1Man_9GlcNAc_2$-RNase (2). A solution of dodecasaccharide oxazoline **4** (1.50 mg, 755 nmol) and GlcNAc-RNase **3** (1.50 mg, 108 nmol) in a phosphate buffer (50 mM, pH 7.0, 50 μL) was incubated with Endo-A mutant N171A (50 μg) at 23 °C. The reaction was monitored by reverse-phase HPLC. After 5 h, the product was purified by HPLC to afford glycoprotein **2** (1.38 mg, 86.5 nmol, 80%). The glycoprotein was quantified with a standard solution of natural RNase by measuring the UV absorbance at 280 nm. Analytical RP-HPLC of **2**, t_R = 21.6 min (see the description in general method for the conditions); ESI−MS of **2**: calcd M = 15 870 Da; Found (*m*/*z*), 1764.45 $[M + 9H]^{9+}$, 1588.25 $[M + 10H]^{10+}$, 1443.95 $[M + 11H]^{11+}$, 1323.71 $[M + 12H]^{12+}$, 1221.99 $[M + 13H]^{13+}$ and 1134.80 $[M + 14H]^{14+}$. Deconvolution of the ESI−MS dada, M = 15 872.0 Da.

Synthesis of Glycoprotein $Man_9GlcNAc_2$-RNase (30). A solution of $Man_9GlcNAc$ oxazoline **29** (500 μg, 0.30 μmol) and GlcNAc-RNase **3** (500 μg, 0.036 μmol) in a phosphate buffer (50 mM, pH 7.0, 20 μL) was incubated with EndoA-N171A (20 μg) at 23 °C for 5 h. The glycoprotein product was isolated by preparative HPLC to give $Man_9GlcNAc_2$-RNase (**30**) as white foam after lyophilization (438 μg, 78%). Analytical RP-HPLC of **30**, t_R = 22 min (see the description in general method for the conditions); ESI−MS of **30**: calcd, M = 15547.0 Da; found, 15548.9 Da (deconvolution data).

Synthesis of Glycoprotein $Glc_1Man_9GlcNAc_2$-RNase (1). Glycoprotein **2** (535 μg, 33.7 nmol) was incubated with β-1,4-galactosidase from *S. pnemoniae* (6 mU) in a phosphate buffer (50 mM, pH 5.5) at 37 °C. The reaction was monitored by ESI−MS. After 2 h, ESI−MS indicated the complete removal of the galactose residue. The product was purified by reverse-phase HPLC to give glycoprotein **1** (530 μg, 33.7 nmol, quantitative). The glycoprotein was quantified with a standard solution of natural RNase B by UV absorbance at 280 nm. ESI−MS of **1**: calcd M = 15 708 Da; Found (*m*/*z*), 1748.23 $[M + 9H]^{9+}$, 1572.01 $[M + 10H]^{10+}$, 1429.19 $[M + 11H]^{11+}$, 1311.4 $[M + 12H]^{12+}$, 1210.72 $[M + 13H]^{13+}$ and 1124.33 $[M + 14H]^{14+}$. Deconvolution of the ESI−MS data, M = 15710.0 Da.

RNase Activity Assay. The ribonuclease activity of the RNase glycoforms was measured by following the method described in the literature.[25] Briefly, a solution (0.5 mg/mL) of yeast RNA (Sigma) in a sodium acetate buffer (500 μL, 100 mM, pH 5.0) was placed in a spectrophotometer. The enzymatic reaction was then initiated by the addition of 2 μg of natural RNase B or each of the individual synthetic glycoforms. The absorbance at 300 nm was recorded in every 2 min. The control reaction was run with the addition of heat-denatured RNase B. The decrease of absorbance at 300 nm over time indicated the progress of degradation of the RNA by the ribonuclease activity.

Circular Dichroism (CD) Spectroscopy. The CD spectroscopic analysis of natural RNase B and the synthetic RNase glycoforms was performed with JASCO 715 instrument at ambient temperature using a 0.1 cm cuvette. Samples were prepared in sodium phosphate buffer (5 mM, pH 7.5) at a concentration of 5−10 μM. The samples were scanned from 260 to 190 at 10 nm/min with a bandwidth of 1 nm and data patching of 0.5 nm. Each spectrum was smoothed and blank subtracted and represented the average of three scans. The data was analyzed using the DICHROWEB server publicly available at online.[23]

Partial and Complete Denaturation of RNase Glycoproteins. The synthetic RNase glycoproteins (**1**, **2**, and **30**) and the natural RNase B (**31**) were denatured following previously reported methods.[27] For partial denaturation without breaking the disulfide bonds, the glycoproteins were dissolved in 0.1 M Tris-HCl buffer (pH 8.5) containing 8 M urea. The solution was incubated at 23 °C for 3 h, and the pH was adjusted to 3.0 by adding HCl. The solution was then dialyzed against 0.1 M acetic acid and the dialyzed solution was lyophilized, which was used for reverse-HPLC analysis and for SPR studies. For complete denaturation, the glycoproteins were incubated with 8 M urea and 0.15 M dithiothreitol (DTT) in a 0.1 M Tris-HCl buffer (pH 8.5) for 3 h. Then, the pH was adjusted to 3.0 and the solution was dialyzed against 0.1 M acetic acid. After lyophilization, the denatured glycoproteins were used for reverse-HPLC analysis and for SPR studies.

Surface Plasmon Resonance (SPR) Measurements. SPR measurements were performed on a Biacore T100 instrument (GE Healthcare). Calreticulin (CRT) was purchased from United States Biological (Swampscott, MA) and was dialyzed against a HEPES buffer (2 mM, pH 7.4) containing 0.5 mM $CaCl_2$ at 4 °C for 16 h to remove Tris buffer in the original sample that would otherwise interfere with the active-ester-based immobilization. Approximately 3000 resonance units (RU) of CRT was immobilized on a CM5 sensor chip in a sodium acetate buffer (10 mM, pH 5.5) at 10 °C, using amine coupling kit provided by the manufacturer. RNase glycoproteins were determined at 10 °C under a flow rate of 30 μL/min. HBS-P+ buffer (10 mM HEPES, 150 mM NaCl, 0.05% surfactant P20, pH 7.4) containing 5 mM $CaCl_2$ was used as sample buffer and running buffer. Association was measured for 2 min and dissociation for 10 min at same flow rate (30 μL/min). The surface regeneration was performed by 0.5% SDS at a flow rate of 10 μL/min for 60 s. The analytes were injected in a concentration of 2 μM, 1 μM, 500 nM, 250 nM, 125 nM, 62.5 nM, and 31.25 nM, respectively. Kinetic analyses were performed by global fitting of the binding data to a 1:1 Langmuir binding model using BIAcore T100 evaluation software and the equilibrium constant K_D was derived. For $Glc_1Man_9GlcNAc_2$-RNase (**1**), $k_{on} = 1.28 \times 10^4\ M^{-1}\ s^{-1}$; $k_{off} = 4.82 \times 10^{-4}\ s^{-1}$; and $K_D = 38$ nM at 10 °C. For $Gal_1Glc_1Man_9GlcNAc_2$-RNase (**2**), $k_{on} = 1.81 \times 10^4\ M^{-1}\ s^{-1}$; $k_{off} = 1.99 \times 10^{-3}\ s^{-1}$; and $K_D = 110$ nM at 10 °C. For a comparative study, the binding of partially denatured and completely denaturated (unfolded) RNase glycoproteins was measured at 250 nM concentration. The denatured $Glc_1Man_9GlcNAc_2$-RNase (**1**) and $Gal_1Glc_1Man_9GlcNAc_2$-RNase (**2**) showed almost the same CRT-binding profiles as those of the corresponding folded glycoproteins, whereas the nonglucosylated $Man_9GlcNAc_2$-RNase (**30**) and $Man_{5-9}GlcNAc_2$-RNase (**31**) did not bind to CRT before and after denaturation.

■ ASSOCIATED CONTENT

Ⓢ Supporting Information. HPLC profile of enzymatic transglycosylation (Figure S1); HPAEC-PAD monosaccharide composition analysis of glycoprotein **2** (Figure S2); reverse-phase HPLC profiles of folded and denatured RNase B (Figure S3); hydrogen-bonding network in the structure of CRT in complex with Glc_1Man_3 tetrasaccharide (Figure S4); and experimental procedures for the synthesis of pentasaccharide **5**. This material is available free of charge via the Internet at http://pubs.acs.org.

■ AUTHOR INFORMATION

Corresponding Author
lwang@som.umaryland.edu

■ ACKNOWLEDGMENT

We thank Dr. Shuang Jake Yang and Dr. Hui Zhang (Johns Hopkins University) for technical assistance in measuring the HRMS (MALDI-TOF) spectra. This work was supported by the National Institutes of Health (NIH grants R01 GM080374 and R01 GM080374-S1).

■ REFERENCES

(1) (a) Helenius, A.; Aebi, M. *Science* **2001**, *291*, 2364–2369. (b) Wang, S.; Ng, D. T. *Nat. Cell Biol.* **2008**, *10*, 251–253. (c) Aebi, M.; Bernasconi, R.; Clerc, S.; Molinari, M. *Trends Biochem. Sci.* **2010**, *35*, 74–82.

(2) Spiro, R. G. *J. Biol. Chem.* **2000**, *275*, 35657–35660.

(3) Zapun, A.; Petrescu, S. M.; Rudd, P. M.; Dwek, R. A.; Thomas, D. Y.; Bergeron, J. J. *Cell* **1997**, *88*, 29–38.

(4) Patil, A. R.; Thomas, C. J.; Surolia, A. *J. Biol. Chem.* **2000**, *275*, 24348–24356.

(5) Kapoor, M.; Srinivas, H.; Kandiah, E.; Gemma, E.; Ellgaard, L.; Oscarson, S.; Helenius, A.; Surolia, A. *J. Biol. Chem.* **2003**, *278*, 6194–6200.

(6) (a) Matsuo, I.; Wada, M.; Manabe, S.; Yamaguchi, Y.; Otake, K.; Kato, K.; Ito, Y. *J. Am. Chem. Soc.* **2003**, *125*, 3402–3403. (b) Arai, M. A.; Matsuo, I.; Hagihara, S.; Totani, K.; Maruyama, J.; Kitamoto, K.; Ito, Y. *ChemBioChem* **2005**, *6*, 2281–2289. (c) Totani, K.; Ihara, Y.; Matsuo, I.; Ito, Y. *J. Biol. Chem.* **2006**, *281*, 31502–31508. (d) Bosis, E.; Nachliel, E.; Cohen, T.; Takeda, Y.; Ito, Y.; Bar-Nun, S.; Gutman, M. *Biochemistry* **2008**, *47*, 10970–10980. (e) Takeda, Y.; Totani, K.; Matsuo, I.; Ito, Y. *Curr. Opin. Chem. Biol.* **2009**, *13*, 582–591. (f) Totani, K.; Ihara, Y.; Tsujimoto, T.; Matsuo, I.; Ito, Y. *Biochemistry* **2009**, *48*, 2933–2940.

(7) Tatami, A.; Hon, Y. S.; Matsuo, I.; Takatani, M.; Koshino, H.; Ito, Y. *Biochem. Biophys. Res. Commun.* **2007**, *364*, 332–337.

(8) (a) Li, B.; Zeng, Y.; Hauser, S.; Song, H.; Wang, L. X. *J. Am. Chem. Soc.* **2005**, *127*, 9692–9693. (b) Zeng, Y.; Wang, J.; Li, B.; Hauser, S.; Li, H.; Wang, L. X. *Chem.—Eur. J.* **2006**, *12*, 3355–3364. (c) Wei, Y.; Li, C.; Huang, W.; Li, B.; Strome, S.; Wang, L. X. *Biochemistry* **2008**, *47*, 10294–10304. (d) Huang, W.; Wang, D.; Yamada, M.; Wang, L. X. *J. Am. Chem. Soc.* **2009**, *131*, 17963–17971. (e) Huang, W.; Groothuys, S.; Heredia, A.; Kuijpers, B. H.; Rutjes, F. P.; van Delft, F. L.; Wang, L. X. *ChemBioChem* **2009**, *10*, 1234–1242. (f) Schwarz, F.; Huang, W.; Li, C.; Schulz, B. L.; Lizak, C.; Palumbo, A.; Numao, S.; Neri, D.; Aebi, M.; Wang, L. X. *Nat. Chem. Biol.* **2010**, *6*, 264–266. (g) Umekawa, M.; Higashiyama, T.; Koga, Y.; Tanaka, T.; Noguchi, M.; Kobayashi, A.; Shoda, S.; Huang, W.; Wang, L. X.; Ashida, H.; Yamamoto, K. *Biochim. Biophys. Acta* **2010**, *1800*, 1203–1209. (h) Huang, W.; Zhang, X.; Ju, T.; Cummings, R. D.; Wang, L. X. *Org. Biomol. Chem.* **2010**, *8*, 5224–5233. (i) Huang, W.; Li, J.; Wang, L. X. *ChemBiochem* **2011**, *12*, 932–941. (j) Rising, T. W.; Claridge, T. D.; Moir, J. W.; Fairbanks, A. J. *ChemBioChem* **2006**, *7*, 1177–1180. (k) Heidecke, C. D.; Ling, Z.; Bruce, N. C.; Moir, J. W.; Parsons, T. B.; Fairbanks, A. J. *ChemBioChem* **2008**, *9*, 2045–2051. (l) Rising, T. W.; Heidecke, C. D.; Moir, J. W.; Ling, Z.; Fairbanks, A. J. *Chem.—Eur. J.* **2008**, *14*, 6444–6464. (m) Parsons, T. B.; Patel, M. K.; Boraston, A. B.; Vocadlo, D. J.; Fairbanks, A. J. *Org. Biomol. Chem.* **2010**, *8*, 1861–1869.

(9) Li, B.; Song, H.; Hauser, S.; Wang, L. X. *Org. Lett.* **2006**, *8*, 3081–3084.

(10) Ochiai, H.; Huang, W.; Wang, L. X. *J. Am. Chem. Soc.* **2008**, *130*, 13790–13803.

(11) Huang, W.; Li, C.; Li, B.; Umekawa, M.; Yamamoto, K.; Zhang, X.; Wang, L. X. *J. Am. Chem. Soc.* **2009**, *131*, 2214–2223.
(12) Huang, W.; Yang, Q.; Umekawa, M.; Yamamoto, K.; Wang, L. X. *ChemBioChem* **2010**, *11*, 1350–1355.
(13) Umekawa, M.; Li, C.; Higashiyama, T.; Huang, W.; Ashida, H.; Yamamoto, K.; Wang, L. X. *J. Biol. Chem.* **2010**, *285*, 511–521.
(14) (a) Umekawa, M.; Huang, W.; Li, B.; Fujita, K.; Ashida, H.; Wang, L. X.; Yamamoto, K. *J. Biol. Chem.* **2008**, *283*, 4469–4479. (b) Wang, L. X.; Huang, W. *Curr. Opin. Chem. Biol.* **2009**, *13*, 592–600.
(15) Heng, L.; Ning, J.; Kong, F. *J. Carbohydr. Chem.* **2001**, *20*, 283–296.
(16) Zhu, Y.; Chen, L.; Kong, F. *Carbohydr. Res.* **2002**, *337*, 207–215.
(17) Matsuo, I.; Isomura, M.; Miyazaki, T.; Sakakibara, T.; Ajisaka, K. *Carbohydr. Res.* **1998**, *305*, 401–413.
(18) Suzuki, K.; Daikoku, S.; Ako, T.; Shioiri, Y.; Kurimoto, A.; Ohtake, A.; Sarkar, S. K.; Kanie, O. *Anal. Chem.* **2007**, *79*, 9022–9029.
(19) Matsuo, I.; Isomura, M.; Miyazaki, T.; Sakakibara, T.; Ajisaka, K. *Carbohydr. Res.* **1997**, *305*, 401–413.
(20) Allen, J. R.; Allen, J. G.; Zhang, X. F.; Williams, L. J.; Zatorski, A.; Ragupathi, G.; Livingston, P. O.; Danishefsky, S. J. *Chem.—Eur. J.* **2000**, *6*, 1366–1375.
(21) (a) Zhang, Y. M.; Mallet, J. M.; Sinay, P. *Carbohydr. Res.* **1992**, *236*, 73–88. (b) Geng, X.; Dudkin, V. Y.; Mandal, M.; Danishefsky, S. J. *Angew. Chem., Int. Ed.* **2004**, *43*, 2562–2565.
(22) Noguchi, M.; Tanaka, T.; Gyakushi, H.; Kobayashi, A.; Shoda, S. I. *J. Org. Chem.* **2009**, *74*, 2210–2212.
(23) (a) Lees, J. G.; Miles, A. J.; Wien, F.; Wallace, B. A. *Bioinformatics* **2006**, *22*, 1955–1962. (b) Whitmore, L.; Wallace, B. A. *Nucleic Acids Res.* **2004**, *32*, W668–673. (c) Lobley, A.; Whitmore, L.; Wallace, B. A. *Bioinformatics* **2002**, *18*, 211–212.
(24) Toumi, M. L.; Go, E. P.; Desaire, H. *J. Pharm. Sci.* **2009**, *98*, 2581–2591.
(25) Kunitz, M. *J. Biol. Chem.* **1946**, *164*, 563–568.
(26) Rudd, P. M.; Joao, H. C.; Coghill, E.; Fiten, P.; Saunders, M. R.; Opdenakker, G.; Dwek, R. A. *Biochemistry* **1994**, *33*, 17–22.
(27) (a) Kumar, T. K.; Gopalakrishna, K.; Ramakrishna, T.; Pandit, M. W. *Int. J. Biol. Macromol.* **1994**, *16*, 171–176. (b) Ristow, S. S.; Wetlaufer, D. B. *Biochem. Biophys. Res. Commun.* **1973**, *50*, 544–550.
(28) (a) Rodan, A. R.; Simons, J. F.; Trombetta, E. S.; Helenius, A. *EMBO J.* **1996**, *15*, 6921–6930. (b) Cannon, K. S.; Helenius, A. *J. Biol. Chem.* **1999**, *274*, 7537–7544.
(29) (a) Saito, Y.; Ihara, Y.; Leach, M. R.; Cohen-Doyle, M. F.; Williams, D. B. *EMBO J.* **1999**, *18*, 6718–6729. (b) Williams, D. B. *J. Cell Sci.* **2006**, *119*, 615–623. (c) Michalak, M.; Groenendyk, J.; Szabo, E.; Gold, L. I.; Opas, M. *Biochem. J.* **2009**, *417*, 651–666.
(30) Ito, Y.; Hagihara, S.; Arai, M. A.; Matsuo, I.; Takatani, M. *Glycoconjugate J.* **2004**, *21*, 257–266.
(31) Kozlov, G.; Pocanschi, C. L.; Rosenauer, A.; Bastos-Aristizabal, S.; Gorelik, A.; Williams, D. B.; Gehring, K. *J. Biol. Chem.* **2010**, *285*, 38612–38620.